Nanosecond Pulse Electroporation of Biological Cells: The Effect of Membrane Dielectric Relaxation

by

Elham Salimi

A Thesis submitted to the Faculty of Graduate Studies of

The University of Manitoba

in partial fulfillment of the requirements for the degree of

Master of Science

Department of Electrical and Computer Engineering

University of Manitoba

Winnipeg, MB, Canada

To my wonderful parents for all their supports.

Abstract

Nanosecond pulse electroporation of biological cells is gaining significant interest due to its ability to influence intracellular structures. In nanosecond pulse electroporation of biological cells nanosecond duration pulses with high frequency spectral content are applied to the cell. In this research we show that accurate modeling of the nanosecond pulse electroporation process requires considering the effect of the membrane dielectric relaxation on the electric potential across the membrane. We describe the dielectric relaxation of the membrane as dispersion in the time-domain and incorporate it into the nonlinear asymptotic model of electroporation. Our nonlinear dispersive model of a biological cell is solved using finite element method in 3-D space enabling arbitrary cell structures and internal organelles to be modeled. The simulation results demonstrate two essential differences between dispersive and nondispersive membrane models: the process of electroporation occurs faster when the membrane dispersion is considered, and the minimum required electric field to electroporate the cell is significantly reduced for the dispersive model.

Acknowledgments

First and foremost, I would like to thank Dr. Greg Bridges, my research advisor, for his help and support. He always provided me with helpful suggestions and ideas to overcome the problems that I encountered along my work.

I thank Microfluidic group for their support and assistance.

I also thank Dr. Douglas Thomson and Francis Lin, my committee members, for their effort to evaluate this work.

I would like to thank my family and friends for their continual support.

Financial support from the Natural Sciences and Engineering Research Council of Canada and the University of Manitoba are greatly acknowledged.

Contents

List of Figures

List of Tables

Chapter 1

Introduction

Electroporation or electropermeabilization is the process of creation of transient hydrophilic pores in the membrane of biological cells upon applying an intense electric field. When a cell is exposed to an external electric field the cell membrane charges up increasing the electric potential across the membrane. Once the required voltage of electroporation is achieved the lipid bilayer molecules of the membrane rearrange themselves and form pores in the membrane through which ions and impermeable molecules can pass and enter the cytoplasm [9–11]. Electroporation is gaining increased importance because of its clinical applications in gene therapy and drug delivery as a method to introduce new DNA and drugs into a cell in order to change its function [12–15]. Electroporation facilitate the cell uptake of impermeable materials.

Conventional methods of electroporation use millisecond to microsecond duration pulses to porate the cell membrane [16,17]. At these time scales the internal and external

cell media behave as good conductors and the electric field is concentrated almost entirely across the cytoplasm membrane leaving the intracellular structures intact. Recently there has been significant interest in investigating the effect of nanosecond and subnanosecond duration pulsed electric fields on the process of electroporation [18–23]. There is evidence that by applying a nanosecond pulsed electric field, such that the rise time of the pulse is less than the charging time of the cell membrane, the electric field can penetrate inside the cell and lead to a different electroporation dynamics called supra-electroporation. In supra-electroporation the intracellular organelle membranes are porated [5, 24, 25].

Despite the numerous experimental studies that have been performed on the conventional and supra-electroporation many aspects of cell electroporation is still unknown due to very small time and spatial scale that the phenomenon occurs. Thus, theoretical and numerical modeling of electroporation is of interest to obtain more insight into the interaction of the external electric field with the cell and the process of pore formation. Linear and nonlinear models of the electrical response of cells to an external electric field have been studied by several research groups [4, 6, 7, 26–29]. In linear models, the electrical parameters of the cell are time independent, whereas in nonlinear models the cell membrane conductivity is not constant and it changes during electroporation. In [6] the linear model of cell is employed to investigate the power dissipated inside the membrane. In [5, 27] the interaction of the applied electric field with the internal structure membrane is studied using the linear model of cell. The nonlinear model of cell is employed in [7, 29] to study

the electroporation of cell in μsec range.

In almost all studies previously performed on the modeling of nanosecond pulse electroporation of cells the cell cytoplasm and membrane are treated as nondispersive media which is adequate for low frequency pulses. However, accurate modeling of nanosecond pulse electroporation of the cell membrane needs to account for the effect of dielectric relaxation of the lipid bilayer molecules of the membrane. In a recent study performed on the effect of the membrane dispersion on the induced transmembrane voltage [30], the authors consider the membrane as a dispersive medium and use the Debye dispersion relation to model it. They calculate the electric potential across the cell membrane, modeled as a linear dispersive medium, when a nanosecond pulsed electric field is applied to the cell. Then they predict the density of the pores created in the membrane by inserting the calculated transmembrane voltage into the asymptotic model of electroporation. Although the method accounts for the effect of the membrane dispersion on the transmembrane voltage it does not incorporate the effect of the instantaneous increase in the membrane conductivity after the creation of pores. In another study performed on the nanosecond pulsed electroporation of cells [4], the authors consider the effect of the pore conduction on the transmembrane voltage by modeling it as a current added to the conduction and displacement currents of the membrane. However, in the proposed model in [4] the membrane is considered as a nondispersive medium. They do the simulations in 2-D space using an active circuit model for the cell membrane.

In this research we describe a nonlinear dispersive model for the membrane to investigate the process of nanosecond pulse electroporation of biological cells. We describe the time-domain implementation of the second order Debye dispersion relation to model the dielectric relaxation of the cell membrane molecules. We then incorporate the dispersion relation into the asymptotic model of electroporation. We perform the simulations in 3-D space employing finite element method implemented in COMSOL Multiphysics.

This thesis begins with a brief introduction on the process of electroporation. The physical and mathematical models of electroporation are discussed in ch. 2. A dispersion model and the electrical models of cell are described in ch. 3 and the cell responses to microsecond and nanosecond pulses are examined in 4. The thesis closes with the conclusion and future work that can extend this research.

Chapter 2

Process of Electroporation

The formation of transient pores inside the membrane of cells using electric fields, called electroporation, has long been investigated due to its applications in cell biology to transform bacteria, plant cells or mammalian cells by loading them with foreign molecules. Experimental studies as well as theoretical modeling of electroporation have been developed to more accurately investigate the process of electroporation and its effects on different types of cells. The application of short duration electric pulses in cell electroporation has caused renewed interest in electroporation studies since intensive short duration pulses are able to penetrate inside the cell and affect the internal organelles.

This chapter begins with an introduction of the physical process of electroporation. Then the conventional method of electroporation and supra-electroporation are compared. Finally the mathematical model of electroporation is introduced.

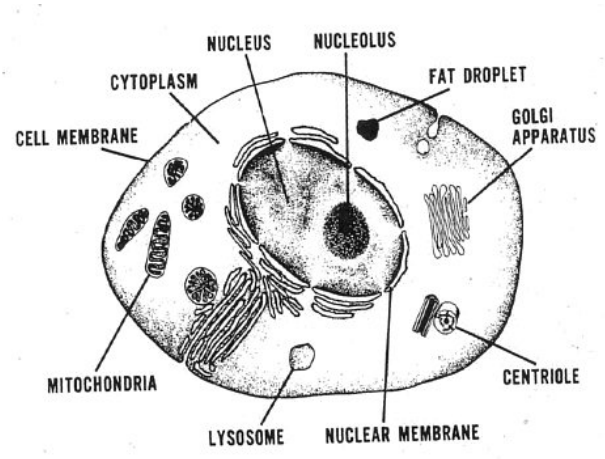

Figure 2.1: *The structure of a eukaryotic cell. All eukaryotic cells have a membrane that isolates the cell interior from the extracellular medium [1].*

2.1 Biological Process of Electroporation

Figure 2.1 shows the structure of a eukaryotic cell. All cells have a membrane that separates the extracellular medium from the cell interior and controls the movement of substances to and out of the cell. The cytoplasm membrane of almost all living cells is made of a lipid bilayer. The phospholipid molecules of the lipid bilayer have a hydrophilic head and a hydrophobic tail (Fig. 2.2). In an intact membrane the phospholipid molecules arrange themselves in a two molecule thick layer such that the hydrophobic tails are towards each other and the hydrophilic heads point out to either sides of the layer. This structure is selectively impermeable to water-soluble substances such as ions and glucose and gives the cell the ability to regulate the transport of materials across the membrane through ion-specific channels, the membrane "pores" [31].

When the cell is exposed to an intense electric field the cell membrane charges up

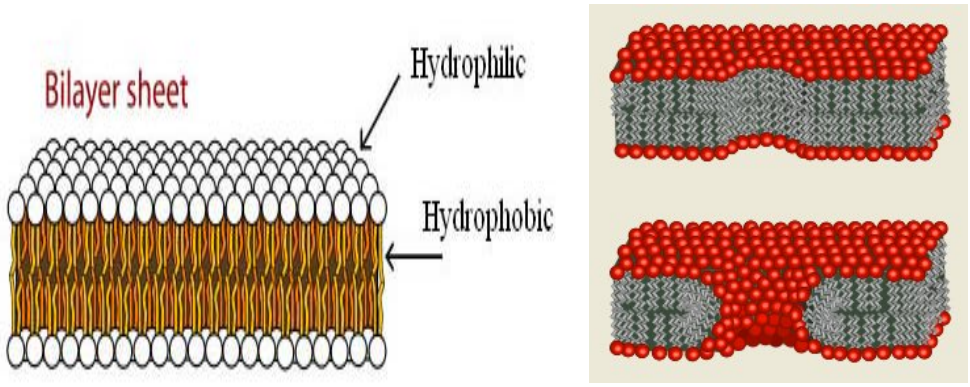

Figure 2.2: *The arrangement of phospholipid molecules of lipid bilayer in (a) an intact membrane [2], and (b) a porated membrane with a hydrophobic pore (Top) and a hydrophilic pore (bottom) [3].*

increasing the electric potential across the membrane. As a result, some transient unstable pores are created in the membrane called "pre-pores" [32]. Pre-pores are hydrophobic since the hydrophobic tails of the phospholipid molecules form the walls. These pores expand and once the radius of them exceed a critical value a rearrangement in phospholipid molecules converts them to stable hydrophilic pores [10]. The structure of hydrophobic and hydrophilic pores are shown in Fig. 2.2. The hydrophilic pores are conductive since they allow polar molecules (e.g. ions, proteins and DNA) to pass across the membrane and enter the cytoplasm. This process is called electroporation and it is reversible or irreversible depending on the intensity of the applied electric field. In the reversible case the pores heal and reseal the bilayer when the electric field is removed, whereas in the irreversible case the pores expand too much, leading to mechanical rupture of the cell membrane [32].

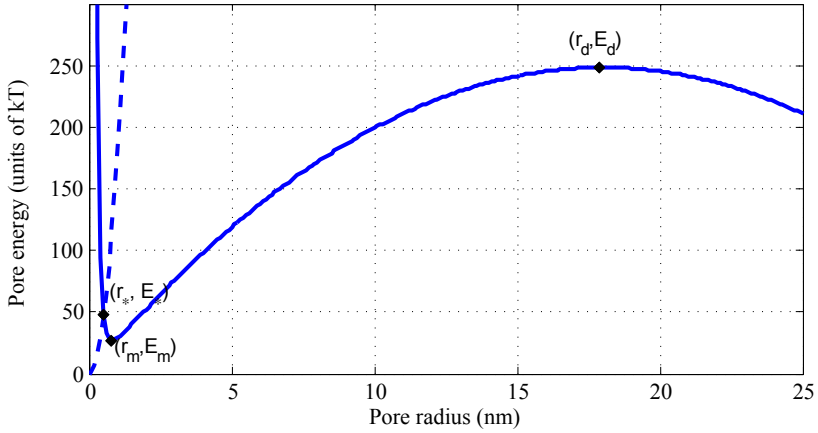

Figure 2.3: *Energy of hydrophobic (dashed line) and hydrophilic (solid line) pores for different pore radiuses.*

Fig. 2.3 shows the energy of hydrophobic and hydrophilic pores at different radiuses. Hydrophobic pores expands until their radius exceed r_* at which the energy of hydrophobic and hydrophilic pores are the same. At this point reorientation of the membrane occurs and the hydrophobic pores are converted to hydrophilic ones. The hydrophilic pore expands to achieve its minimum energy at r_m. If the radius of the pore exceeds r_d the pore expands indefinitely and makes the process of electroporation irreversible [8,10]. More detail about the energy of hydrophobic and hydrophilic pores are given in A

This technique has applications in gene therapy and drug delivery to introduce new DNAs and drugs into a cell. Zeira et al. [15] have used electroporation technique to insert CD4 molecules (the receptor of the Human Immunodeficiency Virus) into red blood cells (RBC). They have shown that RBC-CD4 reduces the load of HIV in uninfected T cells. As an application of electroporation in drug delivery, Mir et al. [14] have combined

chemotherapy and electroporation (electrochemotherapy) to treat tumors. The efficiency of chemotherapy is restricted in tumor treatments because of poor delivery of the drugs into the tumor cells. Bleomycin (BLM) is an impermeable cytotoxic drug which bonds to the cells membrane to affect them. L. They have shown that using electroporation BLM can be loaded into the cell cytoplasm to achieve higher cytotoxicity of the drug. They have shown that electrochemotherapy requires much less concentration of BLM than chemotherapy which reduces the side effects of the drug.

2.2 Conventional and Supra Electroporation

The term "conventional electroporation" refers to formation and expansion of pores with different sizes in the cytoplasm membrane whereas supra-electroporation refers to the creation of extraordinary number of very small pores (not expanding) in both the cytoplasm and intracellular organelles membranes.

Conventional methods of electroporation use long duration electric pulses to electroporate the cells. With long duration electric pulses the electric potential is almost entirely across the membrane since the cytoplasm and the extracellular medium act like good conductors. In this case only the cytoplasm membrane achieves the required voltage to cause the rearrangement of lipid bilayer molecules and the formation of hydrophilic pores. Unlike the conventional electroporation, supra-electroporation employs intensive short duration electric pulses such that the pulse duration is less than the charging time of the

Table 2.1: *The geometrical and electrical parameters of a biological cell with an internal organelle [5].*

Parameter	Symbol	Value
Cell radius	$R1$	10 μm
Cytoplasm membrane thickness	$d1$	5 nm
Organelle radius	$R2$	3 μm
Organelle membrane thickness	$d2$	5 nm
Relative permittivity of the extracellular medium	ϵ_{er}	72
Conductivity of the extracellular medium	σ_e	1.2 S/m
Relative permittivity of the cytoplasm membrane	ϵ_{cmr}	5
Conductivity of the cytoplasm membrane	σ_{cm}	3×10^{-7} S/m
Relative permittivity of the cytoplasm	ϵ_{cr}	72
Conductivity of the cytoplasm	σ_c	0.3 S/m
Relative permittivity of the organelle membrane	ϵ_{omr}	5
Conductivity of the organelle membrane	σ_{om}	3×10^{-7} S/m
Relative permittivity of the organelle interior	ϵ_{or}	72
Conductivity of the organelle interior	σ_o	0.3 S/m

cytoplasm membrane. Short duration electric pulses are able to interact with intracellular structures and cause electroporation of organelles membrane. In supra-electroporation the pores are created with the radius of minimum energy and they do not expand further because with short duration high intensity electric pulses the pore creation dominates the pore expansion. Fig. 2.4 compares the penetration of the electric field inside the cytoplasm of a spherical cell when 100 kV/cm, 10 μs and 100 kV/cm, 10 ns duration pulses are applied to the cell. The geometrical and electrical parameters of the cell are given in Table 2.1 [5]. It is clear that with a 10 μs electric pulse the cytoplasm is like an equipotential area whereas with 10 ns electric pulse the electric field penetrates inside the cytoplasm and causes an electric potential across the internal membrane.

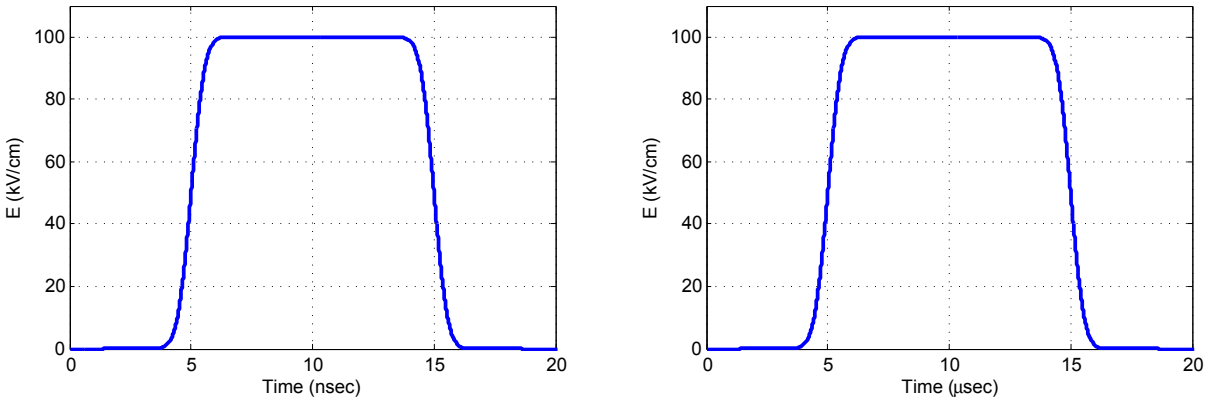

(a) (b)

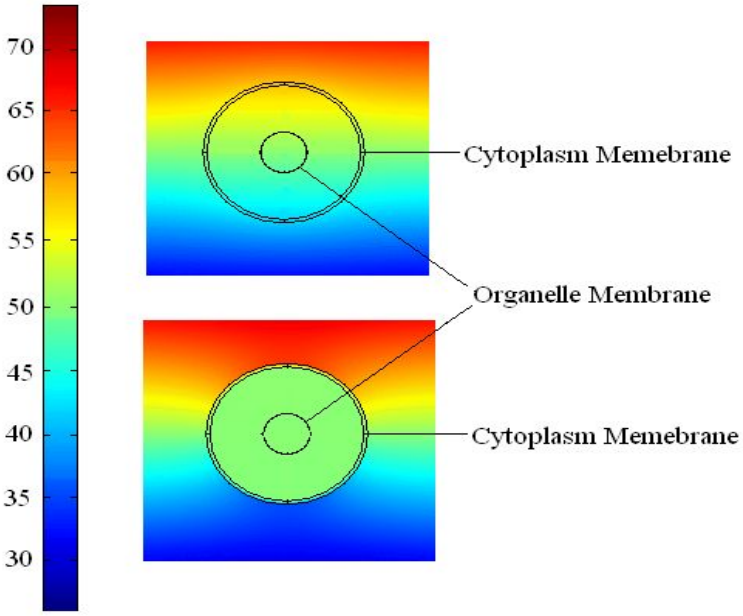

(c)

Figure 2.4: *Penetration of the electric field inside a biological cell when* 10 μs *and* 10 ns *duration electric pulses are applied to the cell. The cell parameters are in Table 2.1 (a)* 10 ns, 100 kV/cm *Gaussian rise-time pulse with* 1 ns *rise-time and fall-time. (b)* 10, μs 100 kV/cm *Gaussian pulse with* 1 μs *rise-time and fall-time. (c) Electric potential inside the cell for the nanosecond (Top) and microsecond (Bottom) pulses. The cell cytoplasm membrane shields the cell interior from the applied microsecond pulsed electric field whereas it allows the nanosecond pulse to penetrate inside the cell.*

There are several studies performed on supra-electroporation since it provides access to the cell internal structure and consequently makes possible the internal manipulation of cells. Kotnik et al. [5] studied a cell with an internal organelle and investigated the electric potential across the internal and external membranes. For a 10 *nsec* duration pulse with 1 *nsec* rise time and fall time they propose that if the organelle membrane has a higher electric conductivity than the cytoplasm or the organelle membrane has lower permittivity than the external membrane then the electric potential difference across the internal membrane may exceed the external membrane. Based on this evidence they conclude that it is possible to electroporate the internal membrane without perturbing the cytoplasm membrane. Although this may be true for some special pulses and electrical parameters, Smith's study [4] shows that in supra-electroporation the internal and external membranes respond in a same manner to the external electric field and they both experience electroporation. Moreover, they explain that using different methods to detect the perturbation of the organelle membrane and the cytoplasm membrane is the reason that some experimental results support the idea of internal membrane electroporation without electroporating the external one [4]. The integrity of the cytoplasm membrane is generally assessed using propidium iodide (PI) which is impermeable to an intact membrane. After the formation of the pores in the membrane PI molecules can pass through the membrane if the pores are wide enough to allow their transport. In supra-electroporation the radius of the pores is very small such that it hinders the PI

molecules transport and consequently suppresses the cytoplasm membrane electroporation. The integrity of the intracellular organelles membrane is assessed by inspecting the concentration change of the internal calcium. The calcium ions are very small that can pass through very small pores created by supra-electroporation. Recent experiments performed by Vernier et al. [33] verify the creation of small pores inside the cytoplasm membrane as well as the intracellular membranes.

2.3 Mathematical Model of Electroporation

The electroporation process, including the formation and expansion of the pores, are described by the Smoluchowski partial differential equation [34]. The Smoluchowski equation defines a pore density function, $n(r,t)$, such that the number of pores with radius between r and $r+dr$ at any given time, t, is $n(r,t)dr$. $n(r,t)$ is described as

$$\frac{\partial n}{\partial t} + D\frac{\partial}{\partial r}\left(-\frac{\partial n}{\partial r} - \frac{n}{kT}\frac{\partial W}{\partial r}\right) = S(r), \tag{2.1}$$

where D is the pore diffusion coefficient, r is the pore radius, W is the formation energy of a pore with radius r, and $S(r)$ describes the transition of hydrophobic pores to hydrophilic ones, as

$$S(r) = \frac{\nu_c h}{kT}\frac{\partial W_o}{\partial r}e^{W_o/kT} - \nu_d n H(r_* - r). \tag{2.2}$$

where ν_c is the pore creation rate, h is the membrane thickness, W_o is the formation energy of a hydrophobic pore, ν_d is the pore destruction rate, r_* is the radius at which hydrophobic and hydrophilic pores have the same energy, and $H(r_* - r)$ is a step function at $r = r_*$.

Assuming that, *(i)* the expansion of the pores is negligible, and *(ii)* the temporal change of the minimum pore energy is negligible, a quasistatic asymptotic model of electroporation simplifies the PDE equation 2.1 to an ordinary differential equation [4, 8]. The ODE defines the pore density, $N(t)$, which is related to $n(r, t)$ as

$$N(t) = \int_{r=0}^{\infty} n(r, t) dr. \tag{2.3}$$

The quasistatic asymptotic equation for $N(t)$ is

$$\frac{dN(t)}{dt} = \alpha e^{(V_m(t)/V_{ep})^2} \left(1 - \frac{N(t)}{N_0} e^{-q(V_m(t)/V_{ep})^2}\right). \tag{2.4}$$

where V_m is the transmembrane voltage, V_{ep} is the characteristic voltage of electroporation, N_0 is the equilibrium pore density at $V_m = 0$, and a and q are constants.

In this project we study the process of electroporation when short duration high intensity pulsed electric fields are applied to the cell. In this situation pores are created faster than they expand making the application of asymptotic model of electroporation valid. As such, in this study we use the asymptotic model of electroporation to study the nonlinear process of electroporation. However, it should be mentioned that as the

duration of the applied pulse approaches the time scale of molecular rearrangement there is an open question on the limit that the asymptotic model of electroporation is valid.

Chapter 3

Electrical models of biological cells

Exposure of cells to an external electric field induces a voltage on the cell membrane called the transmembrane voltage. The value and the spatial distribution of the transmembrane voltage are of significant interest in the electroporation of the cell membrane. Several electrical models have been developed for biological cells exposed to an external electric field to obtain the distribution of the transmembrane voltage. Fig. 3.1 shows a single-shell structure of a spherical cell comprising of the cell cytoplasm and the cell membrane. Here σ_j and ϵ_j define the conductivity and permittivity of each medium with subscripts c,m, and e describing the cell cytoplasm, membrane, and exterior media, respectively. Depending on the definitions of the electrical parameters of the cell we classify the models of the electrical response of cells as linear nondispersive, linear dispersive, nonlinear nondispersive, and nonlinear dispersive. This chapter explains each of these models and the conditions under which they are valid. The chapter begins with an introduction of the

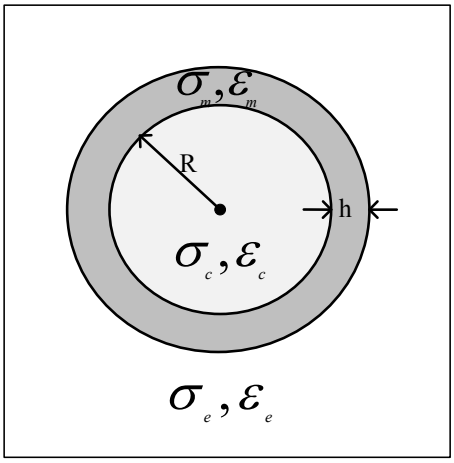

Figure 3.1: *The model of a spherical cell with a single-shell structure. σ_j and ϵ_j are the conductivity and permittivity of each media, respectively.*

Debye dispersion model and its implementation in the frequency-domain and the time-domain. Then the nonlinear modeling of electroporation is discussed and the rest of the chapter focuses on the different models of cells. We mainly focus on the electrical properties of the models and their validity based on the dispersion and nonlinearity concepts. The simulations and discussions on the cell response for each model will be discussed in the next chapter.

3.1 The Debye Dispersion Model

Dispersion is defined through the dependence of the dielectric permittivity of a material on the frequency of the electric field applied. The frequency dependent permittivity reflects the delay in the molecular polarization of the material with respect to the applied alternating electric field. For a linear and isotropic medium the polarization vector is

written as

$$\mathbf{P} = (\epsilon - \epsilon_{\mathbf{0}})\mathbf{E}. \tag{3.1}$$

where ϵ and ϵ_0 are the permittivity of the medium and vacuum, respectively.

In the frequency-domain in order to show the phase delay between the polarization vector and the applied electric field, the permittivity is defined as a complex function of the frequency. The complex permittivity, $\widetilde{\epsilon}$, of a dispersive medium exhibiting an nth order relaxation process can be defined by the Debye dispersion relation as

$$\widetilde{\epsilon} = \sum_{j=1}^{n} \frac{\Delta\epsilon_j}{1 + j\omega\tau_j} + \epsilon_\infty. \tag{3.2}$$

where n is the number of dielectric relaxation steps, τ_j and $\Delta\epsilon_j$ are the time constant and amplitude change of the jth relaxation step and, ϵ_∞ is the medium permittivity at high frequency limit. Equation 3.2 can be separated into real and imaginary parts as

$$\widetilde{\epsilon}(\omega) = \epsilon^{'}(\omega) - j\epsilon^{''}(\omega). \tag{3.3}$$

Here $\epsilon^{'}(\omega)$ is the permittivity of the medium. $\epsilon^{''}(\omega)$ is related to the polarization loss of the medium and it should not be confused with the conductive loss associated with charge carriers.

For nanosecond (1 GHz) models the dielectric relaxation of the cytoplasm and the extracellular medium can be described by a first order Debye relation while a two step

Table 3.1: *Dielectric relaxation parameters of the cell [6]*

	Parameter	Symbol	Value
Cell Membrane	First relaxation time	τ_{m1}	$3 \times 10^{-9}\ s$
	Second relaxation time	τ_{m2}	$4.6 \times 10^{-10}\ s$
	First relaxation amplitude	$\Delta\epsilon_{m1}$	$2.3 \times 10^{-11}\ F/m$
	Second relaxation amplitude	$\Delta\epsilon_{m2}$	$7.4 \times 10^{-12}\ F/m$
	High frequency permittivity	$\epsilon_{m\infty}$	$13.9 \times 10^{-12}\ F/m$
Cell Cytoplasm	Relaxation time	τ_c	$6.2 \times 10^{-12}\ s$
	relaxation amplitude	$\Delta\epsilon_c$	$5.9 \times 10^{-10}\ F/m$
	High frequency permittivity	$\epsilon_{c\infty}$	$1.18 \times 10^{-10}\ F/m$

dielectric relaxation is appropriate for describing the lipid bilayer membrane of biological cells [6]. The first and second relaxations are associated with the headgroup dipoles of the lipid membrane and the water molecules bounded to the membrane surface, respectively [35]. The dielectric relaxation parameters of the cell membrane and cytoplasm are given in Table 3.1 [6]. The dielectric relaxation parameters of the extracellular medium are assumed to be the same as the cytoplasm. Fig. 3.2 shows the frequency dependent behavior of the permittivity and net conductivity, $\sigma_{eff} + \sigma_{m0}$, of the cell membrane and cytoplasm. The dielectric relaxation of the cell cytoplasm occurs at approximately 20 GHz causing an increase in the conductivity and decrease in the permittivity at higher frequencies. Notable decrease in the membrane permittivity and increase in the membrane conductivity occur at frequencies above 20 MHz, leading to high frequency membrane permittivity value 3 times smaller and conductivity value 47 greater than the static values for the membrane permittivity and conductivity, respectively. Therefore, accurate prediction of the membrane electrical response in the frequency range of 20 MH to 1 GHz

requires appropriate definitions of the electrical parameters of the membrane.

Dispersion is accomplished in the time-domain by defining the polarization of the medium as a function of the electric field and its time derivatives [36]. For a second order dispersive medium substitution of (3.3) with $n = 2$ into (3.1) and taking $j\omega$ as the derivative with respect to time yields

$$\begin{aligned} P + (\tau_1 + \tau_2)\frac{\partial P}{\partial t} + \tau_1\tau_2\frac{\partial^2 P}{\partial t^2} \\ = (\epsilon_{m0} - \epsilon_0)E \\ + [(\epsilon_{m0} - \Delta\epsilon_1 - \epsilon_0)\tau_1 \\ + (\epsilon_{m0} - \Delta\epsilon_2 - \epsilon_0)\tau_2]\frac{\partial E}{\partial t} \\ + (\epsilon_{m0} - \Delta\epsilon_1\Delta\epsilon_2 - \epsilon_0)\tau_1\tau_2\frac{\partial^2 E}{\partial t^2}. \end{aligned} \tag{3.4}$$

where ϵ_{m0} is the low frequency permittivity of the membrane.

$$\epsilon_{m0} = \epsilon_\infty + \sum_{j=1}^{2} \Delta\epsilon_j. \tag{3.5}$$

3.2 Nonlinear modeling of Electroporation

As described in the previous chapter, when the transmembrane voltage achieves the required voltage of electroporation some pores are formed in the membrane. The formation of the pores increases the membrane conductivity of the membrane and is electrically

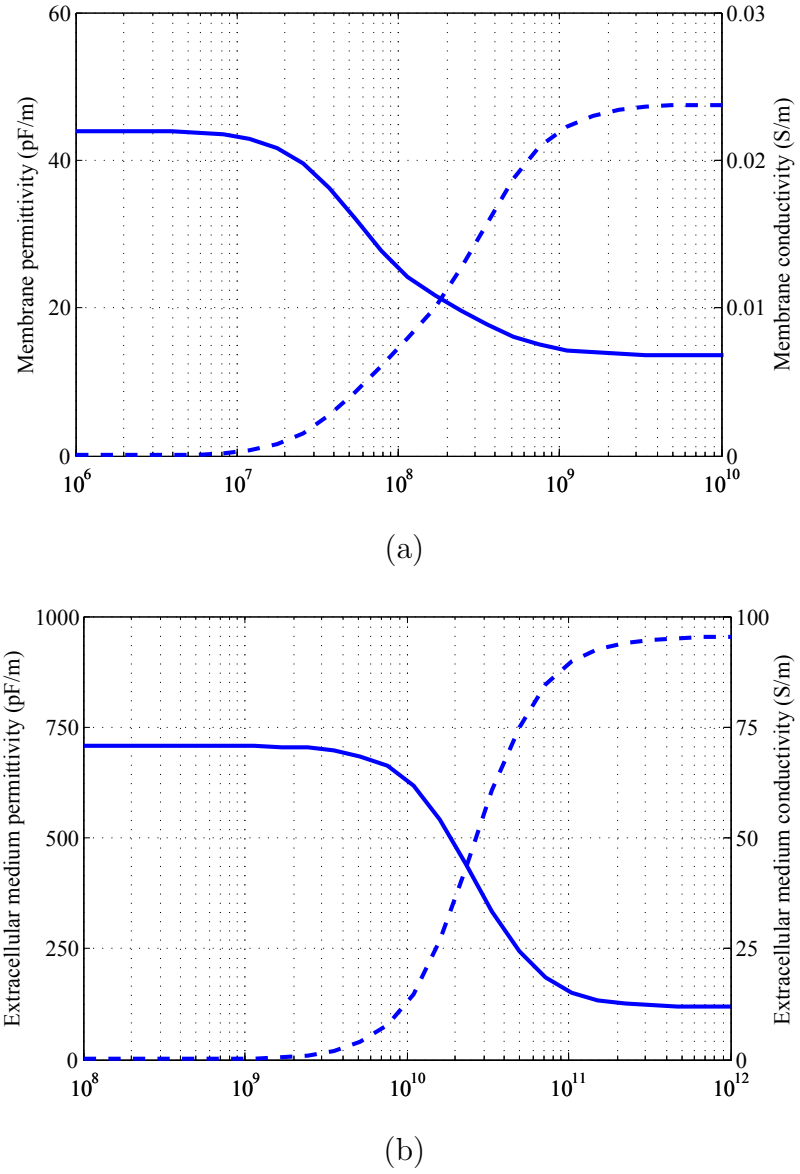

Figure 3.2: *(a) Membrane and (b) Cytoplasm permittivity (solid line), $\epsilon_m^{'}$, and conductivity (dashed line), $\omega\epsilon_m^{''} + \sigma_{m0}$, as functions of frequency.*

modeled as an additional current density, J_{ep}, inside the membrane. J_{ep} is written as

$$Jep(t) = N(t)\frac{\pi {r_p}^2 \sigma_p V_m K}{h}, \tag{3.6}$$

where N is the density of the pores, r_p is the pore radius, σ_p is the conductivity of the solution inside the pore, V_m is the transmembrane voltage, h is the thickness of the membrane, and K is

$$K = \frac{e^{v_m} - 1}{\frac{w_0 e^{w_0 - nv_m} - nv_m}{w_0 - nv_m} e_m^v - \frac{w_0 e^{w_0 + nv_m} + nv_m}{w_0 + nv_m}}. \tag{3.7}$$

In (3.7) w_0 is the energy barrier inside the pore, n is the relative entrance length of the pore, and $v_m = \frac{q_e}{kT} V_m$ is the non-dimensional transmembrane voltage. Assuming that the electric field inside the membrane is uniform, the transmembrane voltage is written as

$$V_m = E_\perp h. \tag{3.8}$$

where $E_\perp$ is the normal electric field.

The pore current density inside the membrane can be translated as an increase in the membrane conductivity using the relation

$$J_{ep} = \sigma_m E_\perp. \tag{3.9}$$

Inserting 3.8 in 3.6 and then the result in 3.9, the conductivity of the membrane at the

points that pores are formed is calculated as

$$\sigma_m(t) = \sigma_{m0} + N(t)\sigma_p \pi {r_p}^2 K, \tag{3.10}$$

where σ_{m0} is the conductivity of the membrane before electroporation. The nonlinearity of the equation 3.10 comes from N which was described in the section 2.3 as

$$\frac{dN(t)}{dt} = \alpha e^{(V_m(t)/V_{ep})^2} \left(1 - \frac{N(t)}{N_0} e^{-q(V_m(t)/V_{ep})^2}\right). \tag{3.11}$$

Under equilibrium conditions (3.10) and (3.11) maintain the transmembrane voltage below the required voltage of electroporation, which is about 1 V. Required voltage of electroporation is the threshold at which notable increase in the density of the pores and membrane conductivity and consequently decrease in the transmembrane voltage occur. The increase in the transmembrane voltage leads to the increase of pore density which lowers the conductivity of the membrane and subsequently the transmembrane voltage. The electroporation parameters for the lipid bilayer membrane of biological cells are given Table 3.2 [7].

Table 3.2: *The electroporation parameters of lipid bilayer membrane [7]*

Parameter	Symbol	Value
Pore creation rate density	α	$1 \times 10^9\ m^2/s$
Characteristic voltage of electroporation	V_{ep}	$170\ mV$
Equilibrium pore density	N_0	$1.5 \times 10^9\ m^{-2}$
Pore creation rate	q	2.46
Pore energy barrier	w_0	2.65
Relative entrance length of pores	n	0.15
Electric charge of an electron	q_e	$1.65 \times 10^{-19}\ C$
Boltzmann constant	k	$1.38 \times 10^{-23} J/K$
Temperature	T	$295\ K$

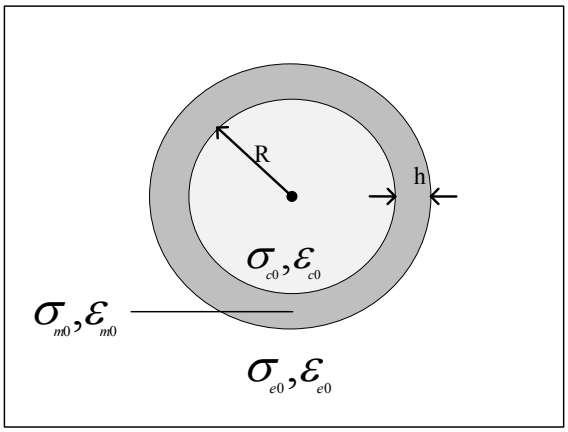

Figure 3.3: *Linear nondispersive model of cell. σ_{i0} and ϵ_{i0} are the static conductivity and permittivity of each medium*

3.3 Cell Models

3.3.1 Linear nondispersive model of cell

In linear nondispersive models the electrical parameters of the cell cytoplasm, membrane, and the extracellular medium are constants as depicted in Fig. 3.3. σ_{i0} and ϵ_{i0} are the static conductivity and permittivity of each medium. Since the electrical parameters are time-invariant the transmembrane voltage calculated from the Laplace equation has a closed form frequency-domain solution [6]

$$V_m = FER\cos\theta \tag{3.12}$$

where E is the strength of the electric field, R is the cell radius, θ is the angle with respect to the electric field, and F is

$$F = \frac{3\Lambda_e\left(3dR^2\Lambda_c + \left(3d^2R - d^3\right)\left(\Lambda_m - \Lambda c\right)\right)}{2R^3\left(\Lambda_m + 2\Lambda e\right)\left(\Lambda_m + \frac{1}{2}\Lambda c\right) - 2(R-d)^3\left(\Lambda_e - \Lambda m\right)\left(\Lambda_c - \Lambda m\right)} \tag{3.13}$$

with

$$\Lambda_e = \sigma_{e0} + j\omega\epsilon_{e0}, \tag{3.14}$$

$$\Lambda_m = \sigma_{m0} + j\omega\epsilon_{m0}, \tag{3.15}$$

$$\Lambda_c = \sigma_{c0} + j\omega\epsilon_{c0}. \tag{3.16}$$

Table 3.3: *The geometrical and electrical parameters of a biological cell modeled as a single-shell structure [7]*

Parameter	Symbol	Value
Cell radius	R	10 μm
Membrane thickness	d	5 nm
Relative permittivity of the extracellular medium	ϵ_{e0r}	80
Conductivity of the extracellular medium	σ_{e0}	0.14 S/m
Relative permittivity of the membrane	ϵ_{m0r}	5
Conductivity of the membrane	σ_{m0}	5×10^{-7} S/m
Relative permittivity of the cytoplasm	ϵ_{c0r}	80
Conductivity of the cytoplasm	σ_{c0}	0.3 S/m

Fig. 3.4 is the graph of the transmembrane voltage vs. frequency for a cell at $\theta = 0$ when the intensity of the applied electric field is 1 kV/cm. The electrical and geometrical properties of the cell are given in Table 3.3 [7]. It is clear that at high frequencies a stronger electric field is required to achieve the transmembrane voltage required for electroporation $(0.7 - 1.5\ V)$.

The time domain response of the cell is calculated from [26]

$$V_m = fER\cos\theta \tag{3.17}$$

where f is obtained from 3.13 by replacing Λ_e, Λ_e, and Λ_e with

$$\Lambda_e = \sigma_{e0} + \epsilon_{e0}\frac{d}{dt} \tag{3.18}$$

$$\Lambda_m = \sigma_{m0} + \epsilon_{m0}\frac{d}{dt} \tag{3.19}$$

$$\Lambda_c = \sigma_{c0} + \epsilon_{c0}\frac{d}{dt}. \tag{3.20}$$

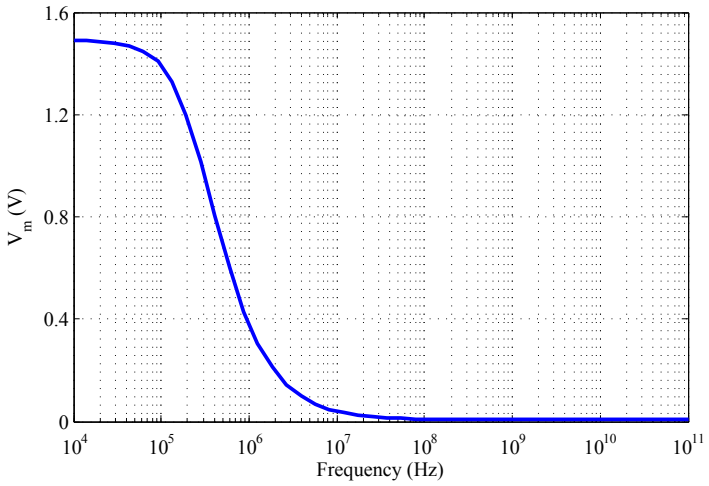

Figure 3.4: *The transmembrane voltage as a function of frequency for the linear nondispersive model of cell.*

The cell response to pulsed electric fields will be discussed in the next chapter.

The linear nondispersive model has been used in several studies due its simplicity. In [5,27] the authors employ the linear nondispersive model for a double shell cell structure to study the interaction of the applied electric field with the internal structure membrane. Kotnik et al. [5] explain that in gigahertz range the electric potential across the organelle membrane can exceed the external membrane provided that the organelle membrane has a higher electric conductivity than the cytoplasm or the organelle membrane has lower permittivity than the external membrane. In another study Kotnik et al. [26] use the linear nondispersive model to investigate the influence of different electric field waveforms on the transmembrane voltage when the cell is kept in physiological ($\sigma = 0.3\ S/m$) and low-conductivity ($\sigma = 0.01\ S/m$) media. They show that with microsecond pulses the

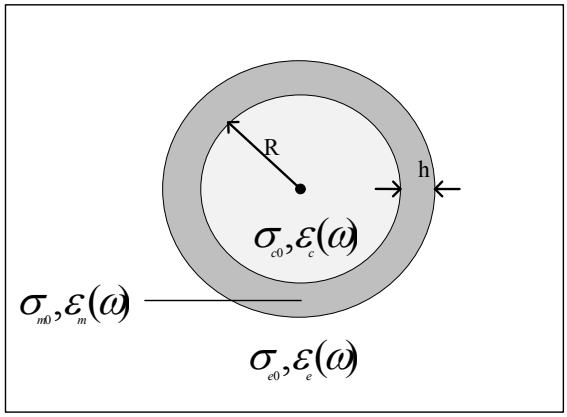

Figure 3.5: *Linear dispersive model of cell. $\epsilon_i(\omega)$ is the frequency dependant permittivity*

shape and amplitude of the transmembrane voltage (time response) are dependent on the conductivity of the extracellular medium.

The linear nondispersive model cannot describe the process of the pores formation inside the membrane nor the dielectric relaxation of the media. Therefore, the model can be adequately used to determine the penetration of low intensity fields (such that the cell membrane is not electroporated) inside the cell at low frequencies (lower than 53 KHz, the dielectric relaxation frequency of the membrane) and even the onset of electroporation.

3.3.2 Linear dispersive model of cell

In the linear dispersive models the conductivity of the cell membrane, cytoplasm and the extracellular medium are constants whereas their permittivity are defined as frequency dependent variables. Fig. 3.5 shows the linear dispersive model of the cell. $\epsilon_e(\omega)$, $\epsilon_m(\omega)$,

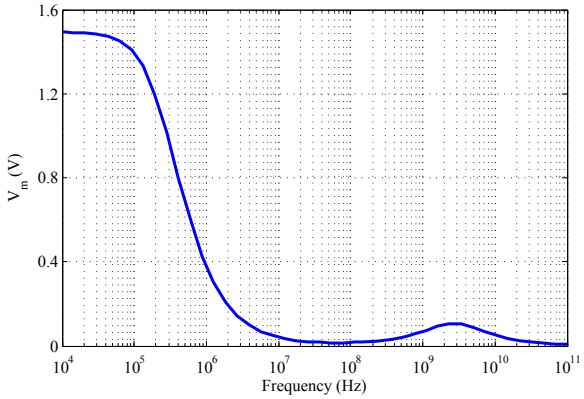

Figure 3.6: *The transmembrane voltage as a function of frequency for the linear dispersive model of cell.*

and $\epsilon_c(\omega)$ are defined using the Debye dispersion relation as

$$\epsilon_m(\omega) = \epsilon_{m\infty} + \frac{\Delta\epsilon_{m1}}{1 + j\omega\tau_{m1}} + \frac{\Delta\epsilon_{m2}}{1 + j\omega\tau_{m2}}, \tag{3.21}$$

$$\epsilon_e(\omega) = \epsilon_c(\omega) = \epsilon_{c\infty} + \frac{\Delta\epsilon_c}{1 + j\omega\tau_c}. \tag{3.22}$$

with parameters given in Table 3.1.

The frequency domain response of the cell is obtained from 3.12 by replacing ϵ_{e0}, ϵ_{m0}, and ϵ_{c0} by $\epsilon_m(\omega)$, $\epsilon_e(\omega)$, and $\epsilon_c(\omega)$ defined in 3.22 [6]. Fig. 3.6 is the graph of the transmembrane voltage vs. frequency for a cell (parameters given in Table 3.3) at $\theta = 0$ when the intensity of the applied electric field is 1 kV/cm. The transmembrane voltage at low frequencies is the same as linear dispersive model. However, at frequencies above 50 MHz it shows a different behavior due to changes in the permittivity and conductivity of the membrane.

For accurate prediction of the transmembrane voltage due to pulses with high frequency spectral content the dielectric relaxations of the three media are required to be accounted for. However, the dielectric relaxation of the cytoplasm and suspending medium occur at frequencies approaching 20 GHz [6], which is beyond the frequency spectrum of nanosecond pulses considered in this work. Therefore, in the transmembrane voltage calculation the membrane is the only dispersive medium and the cytoplasm and the suspending medium are treated as nondispersive media.

In order to calculate the transmembrane voltage in the time-domain, we use the time-domain implementation of the Debye dispersion relation defined in 3.4. We solve the Laplace equation

$$-\nabla \cdot \frac{\partial}{\partial t}\left(\epsilon_0 \nabla V_m + P\right) - \nabla \cdot \sigma_{m0} \nabla V_m = 0, \tag{3.23}$$

in conjunction with 3.4, the partial differential equation of the polarization vector.

The linear dispersive model extends the valid frequency range of the previous model to 20 GHz at which the dielectric relaxation of the cytoplasm occurs. Since the model is linear it fails to predict the formation of the pores and can be used in low intensity electric field studies such that the cell membrane is not electroporated. There are several studies performed on linear nondispersive model of cell. Merla uses the linear nondispersive model to study the effect of the membrane dielectric relaxation on the transmembrane voltage. She then inserts the calculated transmembrane voltage into the pore density equation 3.11 to investigate the effect of the membrane dispersion on the density of the pores created

inside the membrane [30]. Kotnik et al. use the model to study the power dissipation of the membrane at high frequencies [6]. They theoretically show that at high frequencies the power dissipated within the membrane exceeds that of the external medium if the dielectric relaxation of the membrane is considered.

3.3.3 Nonlinear nondispersive model of cell

In nonlinear nondispersive models the permittivity and conductivity of the cell cytoplasm and the extracellular medium and the permittivity of the membrane are constants whereas the membrane conductivity is an E-field dependent (and thus time varying for transient fields) variable. Fig. 3.7 shows the linear dispersive model of cell. $\sigma_m(t)$ is the time dependant membrane conductivity described in 3.10.

The transmembrane voltage is calculated by solving the Laplace equation

$$-\nabla \cdot \frac{\partial}{\partial t}\left(\epsilon_{m0} \nabla V_m\right) - \nabla \cdot \sigma_m \nabla V_m = 0, \tag{3.24}$$

in conjunction with 3.10 and 3.11. In the nonlinear nondispersive model of the cell pores are formed in the membrane at the points that the required voltage of electroporation is achieved and causes an instantaneous increase in the membrane conductivity and consequently decrease in the transmembrane voltage. Thus, the nonlinear nondispersive model is applicable in high intensity electric fields. However, in the model the dielectric relaxation of the membrane is not considered. Therefore, the model is valid only when low

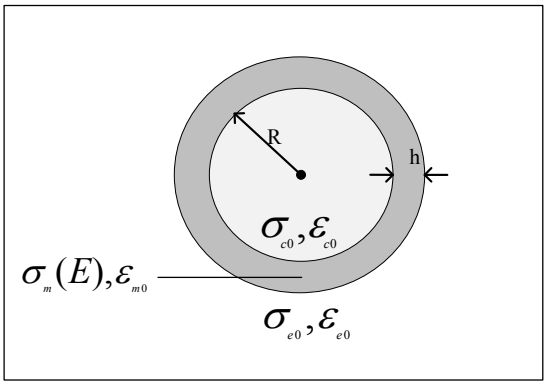

Figure 3.7: *Nonlinear nondispersive model of cell. $\sigma_m(E)$ is the time dependant membrane conductivity.*

frequency electric pulses are applied to the cell.

The nonlinear nondispersive model can be adequately used to predict the transmembrane voltage and the parts of the cell that experience electroporation when low frequency electric pulses are applied to the cell. Kotnik et al. [7] employ the nonlinear nondispersive model to study the transmembrane voltage in an irregularly shaped cell when a 1 kV/cm step electric field is applied to the cell. In their simulations the cell electroporation occurs after 1 μsec because the intensity of the applied electric field is not sufficiently high to electroporate the cell in nanosecond range. Their finite element simulation results performed in 3-D space show good agreement with the experiments at the regions of the cell that experience electroporation. In [4, 19] Smith employs the nonlinear nondispersive model to investigate the process of electroporation for a cell with internal structures when nanosecond pulsed electric fields are applied to the cell. They perform the sim-

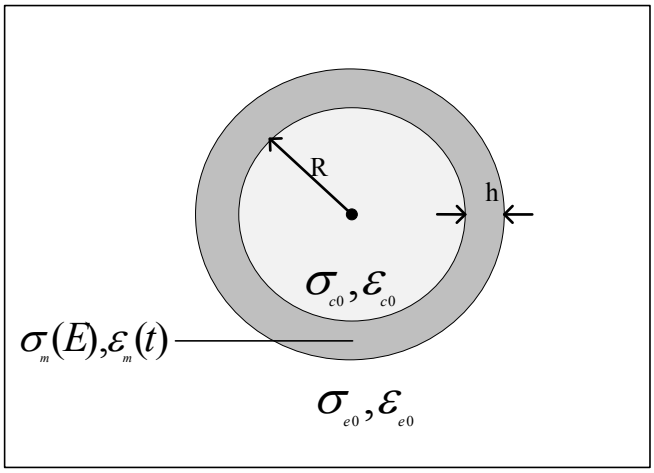

Figure 3.8: *Nonlinear dispersive model of cell. $\sigma_m(E)$ and $\epsilon_m(t)$ are the field and time dependant membrane conductivity and permittivity.*

ulations in a 2-D space using passive circuit elements to model the cytoplasm and the extracellular medium and active elements to model the membranes. Their simulations show supra-electroporation in the internal membranes as well as the cytoplasm membranes. In another study Hu and Joshi use the nonlinear nondispersive model to study the transmembrane voltage in a spheroidal shape cell [23]. The simulations performed on oblate and prolate spheroidal cells shows substantially higher transmembrane voltage for the oblate cells. Based on this evidence they propose pre-orientating the spheroidal cells before applying an external electric field for optimal uptake of drug, DNA, or other substances in experimental studies.

3.3.4 Nonlinear dispersive model of cell

In the nonlinear dispersive model of the cell the electrical parameters of the cell cytoplasm and extracellular medium are assumed constant (for ns-...) whereas the conductivity of the membrane is field dependent and the permittivity of the membrane is time dependent. Fig. 3.8 shows the nonlinear dispersive model of a cell. $\sigma_m(E)$ is the membrane conductivity defined in Eq. 3.10 and $\epsilon m_(t)$ is the time-domain version of the membrane permittivity described in 3.21. As described in the section 3.1 the time-domain implementation of the Debye dispersion relation can be accomplished by defining the polarization vector of the membrane as 3.4. The transmembrane voltage is calculated by solving the Laplace equation

$$-\nabla \cdot \frac{\partial}{\partial t}\left(\epsilon_0 \nabla V_m + P\right) - \nabla \cdot \sigma_m \nabla V_m = 0, \tag{3.25}$$

in conjunction with Eqs. (3.11), (3.10), and (3.4). The form of the Laplace equation shows that both the conduction current of the porated regions and membrane dispersion play roles in determining the transmembrane voltage.

The nonlinear dispersive model is capable of predicting the formation of the pore density on the membrane as well as the dielectric relaxation of the membrane. As such, it can be employed when high intensity and high frequency content electric pulses (up to 20 GHz when the dielectric relaxation of the cytoplasm and extracellular media become

important) are applied to the cell. The nonlinear dispersive model is the most accurate model to investigate the process of nanosecond pulse electroporation of biological cells.

To my knowledge there is no study reported on the nonlinear dispersive model of the cell. We study the nonlinear dispersive response of cell to microsecond and nanosecond pulses in more detail in the next chapter.

In all the described models we used Laplace equation to calculate the transmembrane voltage. The application of the Laplace equation is valid here because the time required for the electric field to pass through a biological cell is typically in the range of femtoseconds, which is much smaller than the rise-time of the pulses applied in cell electroporation.

Chapter 4

Simulation Results

The electroporation of cells occur when the cells are exposed to strong electric fields. Modeling of the interaction of the external electric field with the cell is of special importance since it helps with better understanding of the electroporation process. The cell electrical model plays an important role on the modeling electric response of cell to an external electric field. As discussed in ch. 3 there are four electrical models for a cell based on the electrical parameters of the cell. In this chapter we study the dynamic response of the described models to microsecond and nanosecond pulsed electric fields. The chapter begins with a brief introduction on the numerical model employed in the study. Then the simulation results on microsecond and nanosecond response of cell are presented with more focus on the nonlinear dispersive model. Finally the effect of the pulse duration on the temporal response of cell is discussed.

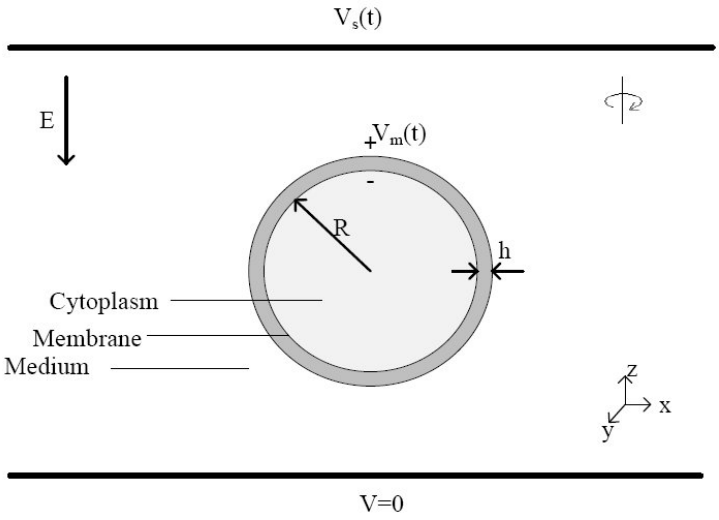

Figure 4.1: *The geometry of a single-shell cell in a lossy medium. The top and bottom faces of the calculation block are taken as the electrodes to which electric voltages are applied. The electrodes are 100* μm *apart.*

4.1 3-D model of cell in COMSOL Multiphysics

We employ the finite element based software COMSOL Multiphysics 3.5 to simulate the response of cells to applied electric pulses. Fig. 4.1 shows the geometry of the spherical single-shell cell embedded in a lossy medium that we employ for our simulations. The cell parameters given in Table 3.3 have been previously used in [7] and they are chosen to match with Chinese hamster ovary cells (CHO). The cell radius is 10 μm and the thickness of the cell membrane is 5 nm. In our numerical model the cell is embedded in a 3D 100 μm^3 simulation space. An electric potential, $V_s(t)$, is applied to the upper plane of the simulation space and the lower plane is set to ground potential. The electric potential at

any point is calculated by solving the Laplace equation

$$-\nabla \cdot \frac{\partial}{\partial t}\left(\epsilon_{\mathbf{0}} \nabla \phi + P\right) - \nabla \cdot \sigma \nabla \phi = \mathbf{0}, \tag{4.1}$$

with

$$E = -\nabla \phi. \tag{4.2}$$

The auxiliary equations 3.11, 3.10, and 3.4 accompany 4.1 where required. The transmembrane voltage at any point on the cell membrane is calculated as the difference between the electric potential at the outer and inner surfaces of the membrane

$$V_m = \phi|_{r+h} - \phi|_r. \tag{4.3}$$

We use the Quasistatics-Electric Currents application mode to solve the Laplace equation 4.1, the PDE Modes-Weak Form Boundary application mode to solve the pore density equation 3.11, and the PDE modes-Coefficient form to solve the polarization vector equation 3.4. The Laplace equation is solved at the subdomains inside the cell, membrane, and outside the cell (simulation box), the pore density equation is solved on the surface of the membrane, and the polarization vector equation is solved inside the membrane subdomain. The initial value of all the variables are set to zero at $t = 0$ except for the initial density of the pores on the membrane which is set to N_0, the equilibrium pore density. *Direct PARADISO* solver is used to solve the equations.

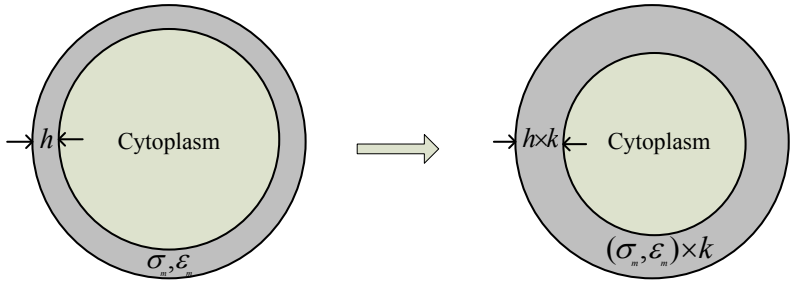

Figure 4.2: *Scaling the thickness of the membrane. The electrical parameters of the membrane are scaled as well to maintain the transmembrane voltage as before scaling.*

In our model the thickness of the membrane is more than 1000 times smaller than the cell radius which makes the numerical solution complicated and time consuming. Kotnik et al. have addressed the problem by replacing the membrane with a current boundary condition that accounts for the membrane conduction and displacement currents and the pores conduction after electroporation of the membrane [7]. This method is efficient in memory and time. However, it cannot be improved to incorporate more features inside the membrane. Since the membrane has a smooth radius of curvature, in our simulations we employ a geometrical scaling to the thickness of the membrane to avoid numerical complication [37, 38]. In order to maintain the electric field inside the membrane and the transmembrane voltage as before scaling the electrical parameters of the membrane are scaled as well, as shown in Fig. 4.2.

We verify the thickness scaling method by simulating the thick and thin membrane cell response to an external electric field and comparing the transmembrane voltage, normal electric field and tangential electric field inside the membrane, as shown in Fig. 4.3. The

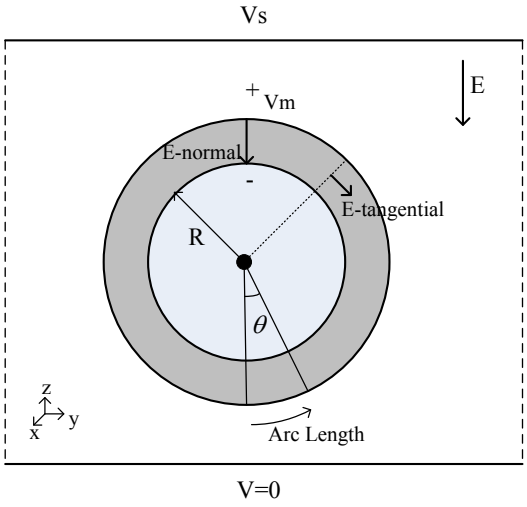

Figure 4.3: *The transmembrane voltage, normal and tangential electric fields inside the membrane*

simulations are done on the linear nondispersive model of the cell when a step voltage of 10 V is applied to the top electrode. Figures 4.4 and 4.5 are the plots of the transmembrane voltage and the normal and tangential electric fields inside the thick and thin membranes 100 $nsec$ and 10 $usec$ after the onset of the electric field. A scaling factor of 100 is employed in the simulations. The results of the thick membrane model are in good agreement with the thin membrane one with maximum error of 10 percent. Regarding the error of less than 10 percent, we use the scaled model to study the process of electroporation. The scaling technique enables further investigations on the mechanical properties of the pores as well as modeling other fine features in the membrane.

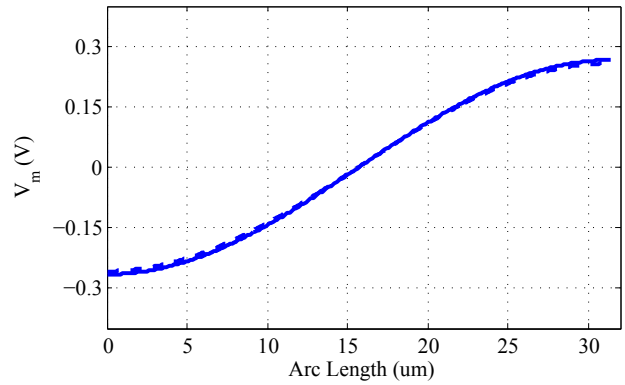

(a)

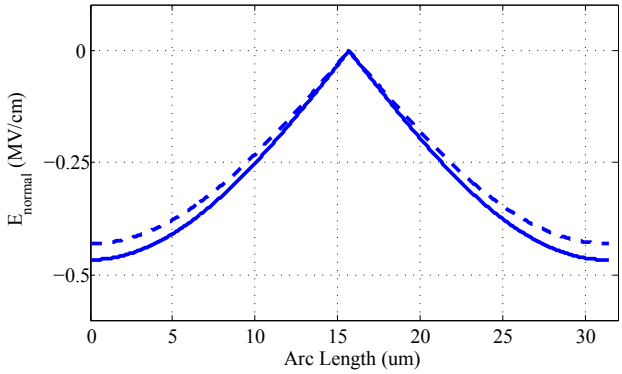

(b)

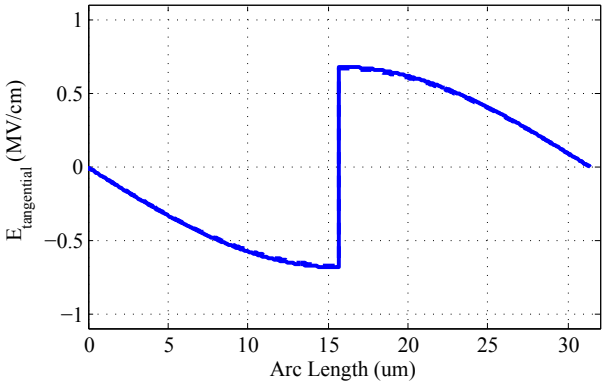

(c)

Figure 4.4: *Comparison of (a) the transmembrane voltage, (b) the normal electric field, and (c) the tangential electric field inside the actual and scaled membrane* 100 *nsec after the onset of the electric field. The horizontal axis is the arc length around the cell starting from the bottom point on the cell.*

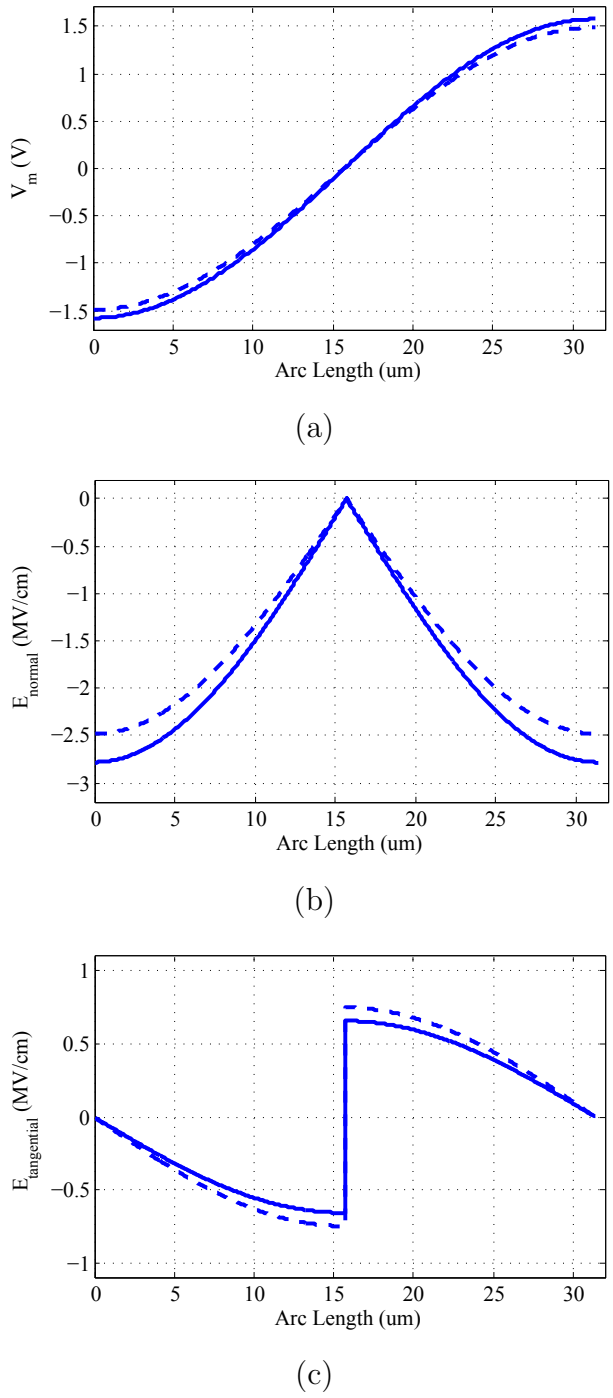

Figure 4.5: *Comparison of (a) the transmembrane voltage, (b) the normal electric field, and (c) the tangential electric field inside the actual and scaled membrane* 10 μ*sec after the onset of the electric field. The horizontal axis is the arc length around the cell starting from the bottom point on the cell.*

4.2 Time-Domain Dispersion Model Verification

Before we proceed to incorporate the dispersion relation into the nonlinear model of electroporation, we verify the time-domain dispersion relation by comparing the time-domain and frequency-domain response of the cell when a single frequency sinusoidal electric field is applied to the cell. The linear dispersive model of the cell is implemented in both the time-domain and the frequency-domain using equations (3.11) and (3.4), respectively. Sinusoidal electric fields in the frequency range of 10 kHz to 1 GHz are applied to the time-domain model of the cell and the amplitude and phase of the transmembrane voltage at the top of the cell is compared with the frequency-domain response at each frequency. The results, depicted in Fig. 4.6, show the time-domain and frequency-domain response match within 1% error.

4.3 Cell response to nanosecond pulses

We apply a nanosecond duration Gaussian pulsed voltage to the top electrode producing an electric field of 65 kV/cm intensity across the cell at its peak (Fig. 4.7). The $10-90\%$ rise-time of the applied pulse is 0.7 $nsec$ and it has a full width at half maximum (FWHM) of 0.94 $nsec$. With nanosecond electric pulses the electric response of the cell is effectively determined by the dielectric properties of the cytoplasm, membrane, and extracellular medium because of the high frequency spectral content of the pulse.

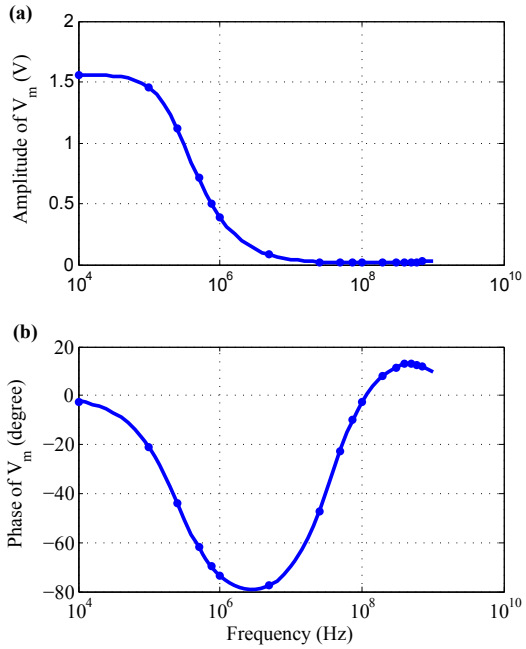

Figure 4.6: *Transmembrane voltage at the top of the cell to compare the Debye dispersion relation in the frequency-domain (solid line) with the time-domain implementation (marked points). (a) Amplitude and (b) Phase of the transmembrane voltage.*

Therefore, we expect to observe different behaviors for the dispersive and nondispersive models since the permittivity of the membrane is highly influenced by the membrane dielectric relaxation. The dispersion equation (3.2) predicts lower permittivity for the membrane for high frequency components of the applied pulse. Thus, the membrane capacitance in the dispersive model is smaller than that of the nondispersive one which results in higher transmembrane voltage in the dispersive model.

Most of numerical studies previously performed on nanosecond pulsed electroporation of cells have employed trapezoidal pulse waveforms as the electroporating signal (Fig. 4.8 shows the pulse used in [4]). The sharp discontinuities in the trapezoidal waveform contain high frequency components which are filtered in real experiments, but in simulations result

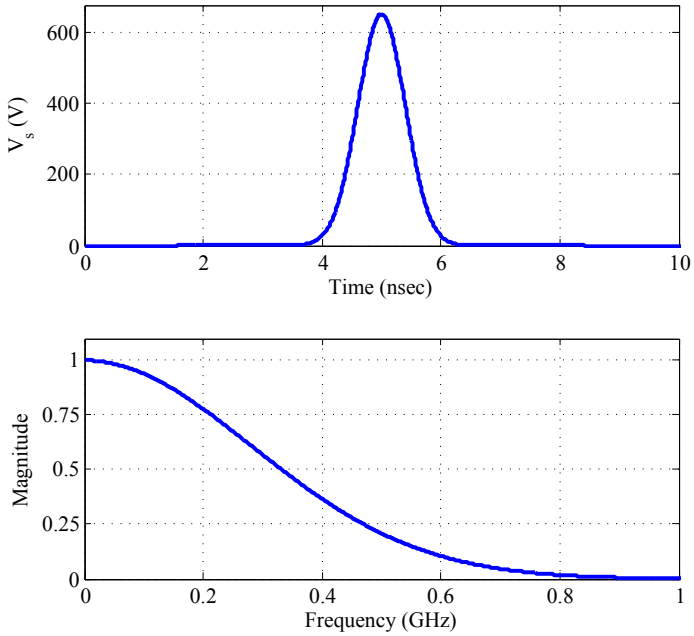

Figure 4.7: *Applied nanosecond Gaussian pulsed voltage and its frequency spectral content. The* $10-90\%$ *rise-time of the pulse is* 0.7 *nsec and the peak is at* 5 *nsec. The rise-time of the pulse is chosen such that the pulse has enough energy at the frequencies that dispersion occurs for biological cells membrane.*

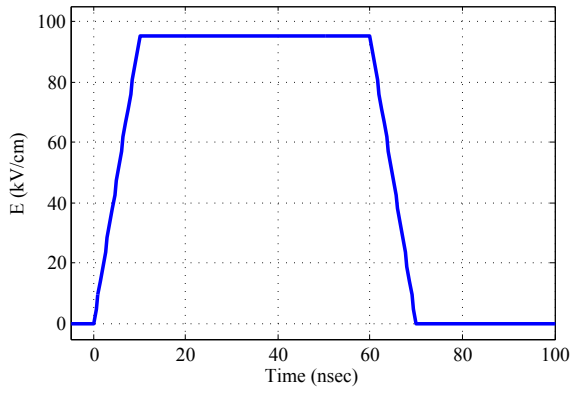

Figure 4.8: *The trapezoidal pulse waveform used in [4].*

in unnatural artifact points in the cell electrical response. A smooth Gaussian shaped pulse, with nanosecond parameters similar to that in [24], is employed in this study.

4.3.1 Linear model response

Fig. 4.9 shows the transmembrane voltage along the circumference of the cell for the linear dispersive and nondispersive models. The transmembrane voltage around the cell has a sinusoidal shape with the maximum and minimum at the top and bottom of the cell, respectively. The transmembrane voltage at any point on the membrane follows the pattern of the applied electric field. The membrane charges increasing the transmembrane voltage until the peak of the pulse is achieved. Afterwards the transmembrane voltage decreases as the applied electric field goes down. As expected the dispersive model predicts a higher transmembrane voltage than the nondispersive model at any point on the membrane. The linear models do not consider the creation of the pores and increase in the membrane conductivity. Thus, the transmembrane voltage can increase infinitely and may exceed the required voltage of electroporation.

The time response of the transmembrane voltage and normal polarization at the top point of the cell are shown in Fig. 4.10. The transmembrane voltage has the shape of the applied electric pulse at the rising edge of the pulse. However, for the dispersive membrane it does not reach zero at the end of the pulse because of the slow discharging response of the membrane. The dispersive membrane response is faster because the membrane time

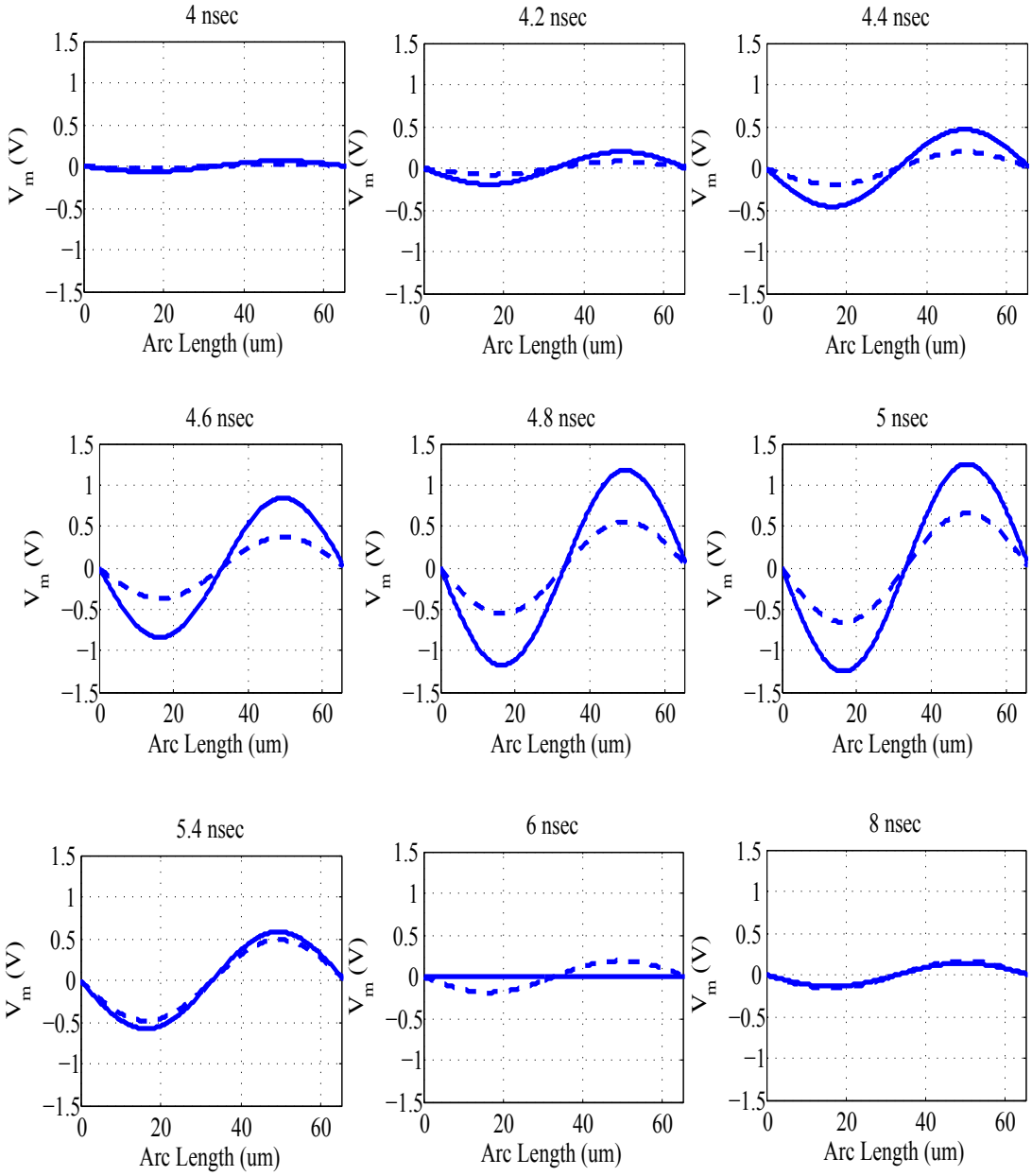

Figure 4.9: *The transmembrane voltage around the cell circumference starting from the right most point on the equator and moving clockwise for the linear dispersive (solid line) and nondispersive (dashed line) models when a* 65 kV/cm *nanosecond electric field is applied to the cell.*

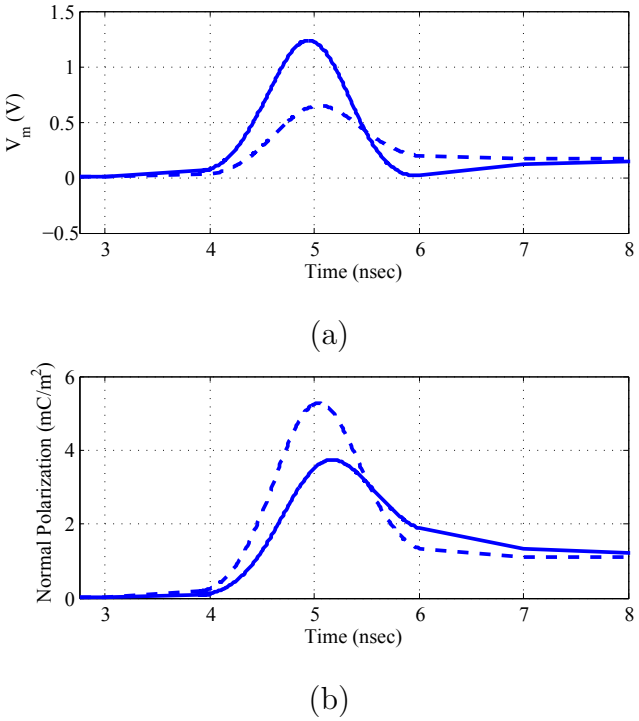

Figure 4.10: *Time course of (a) the transmembrane voltage and (b) the normal polarization at the top of the cell when a nanosecond electric field of* 65 *kV/cm is applied to the linear model of the cell.*

constant (ϵ/σ) is smaller due to lower membrane permittivity. The lower level of P for the dispersive model verifies the lower membrane capacitance and consequently higher voltage drop across the membrane.

4.3.2 Nonlinear model response

Fig. 4.11 shows the transmembrane voltage along the circumference of the cell for the dispersive and nondispersive models when the pulse shown in Fig. 4.7 is applied to the cell. The transmembrane voltage at each point on the membrane follows the pattern of the applied electric field until the required voltage of electroporation is achieved. The top and

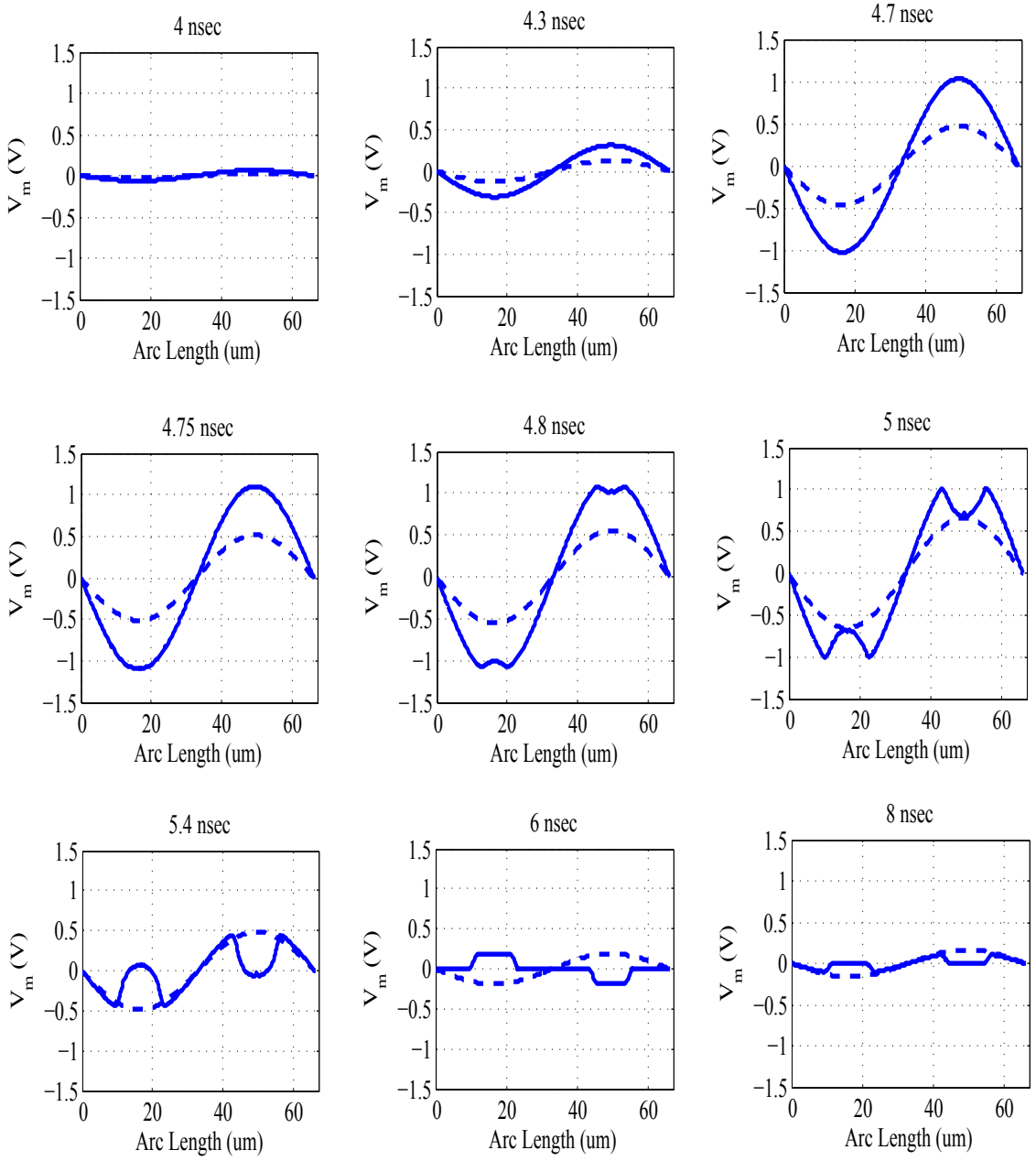

Figure 4.11: *The transmembrane voltage along the cell circumference starting from the right most point on the equator and moving clockwise for the nonlinear dispersive (solid line) and nondispersive (dashed line) models when a* 65 *kV/cm nanosecond electric field is applied to the cell. The top and bottom of the cell close to the electrodes are electroporated in the dispersive model.*

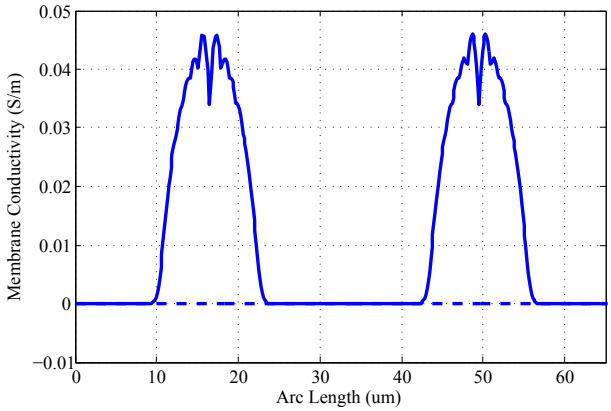

Figure 4.12: *The conductivity of the membrane at $t = 5$ nsec along the cell circumference starting from the right most point on the equator and moving clockwise for the nonlinear dispersive (solid line) and nondispersive (dashed line) models when a 65 kV/cm nanosecond electric field is applied to the cell.*

bottom of the cell facing the electrodes are the first spots that experience electroporation. When the pores are formed, the conductivity of the membrane increases rapidly resulting in lower transmembrane voltage. After this the electroporated area increases as the pulse proceeds to its peak. The onset of electroporation occurs after 4.75 $nsec$ for the dispersive model, whereas for the nondispersive model the electric field is not sufficiently strong to electroporate the cell. The essential difference between the dispersive and nondispersive models is that $V_{m|dispersive} > V_{m|nondispersive}$ at each time step due to lower membrane capacitance for the dispersive model. Fig. 4.12 is a plot of the membrane conductivity around the circumference of cell at $t = 5$ $nsec$, illustrating the regions on the cell that experience electroporation. It is obvious that the pole areas of the dispersive model are electroporated.

The time response of the transmembrane voltage, normal polarization, pore density,

and membrane conductivity at the top point of the cell are shown in Fig. 4.13. The transmembrane voltage starts increasing faster for the dispersive membrane. Therefore, the required voltage of electroporation is achieved after 4.75 *nsec* while the maximum transmembrane voltage achieved for the nondispersive model is at the peak of applied pulse. Fig. 4.13 shows distinctly different transmembrane behavior at the falling edge of the pulse for the dispersive and nondispersive models. It is interesting to observe that in the dispersive model the transmembrane voltage at polar regions obtains negative values and then approaches zero after 7 *nsec*, while in the nondispersive model the transmembrane voltage approaches zero after 30 μsec (not shown) remaining positive all the time. The essential difference is that the time constant (ϵ/σ) of the membrane is much smaller for the dispersive model as the result of the increase in the membrane conductivity due to electroporation and decrease in the membrane permittivity due to the dielectric relaxation of the membrane. The time constant of the membrane is approximately 200 *psec* for the dispersive membrane whereas it is 80 μsec for the nondispersive one. Since the fall time of the applied electric pulse is 700 *psec* the electroporated dispersive membrane has sufficient time to discharge while the cytoplasm remains charged due to slower response (the time constant of the cytoplasm is approximately 2.5 *nsec*). Therefore, the cytoplasm charges the membrane in the opposite direction causing a negative transmembrane voltage in the dispersive model. The time course of the polarization vector shows weaker polarization for the dispersive model which results in lower transmembrane voltage. As depicted in

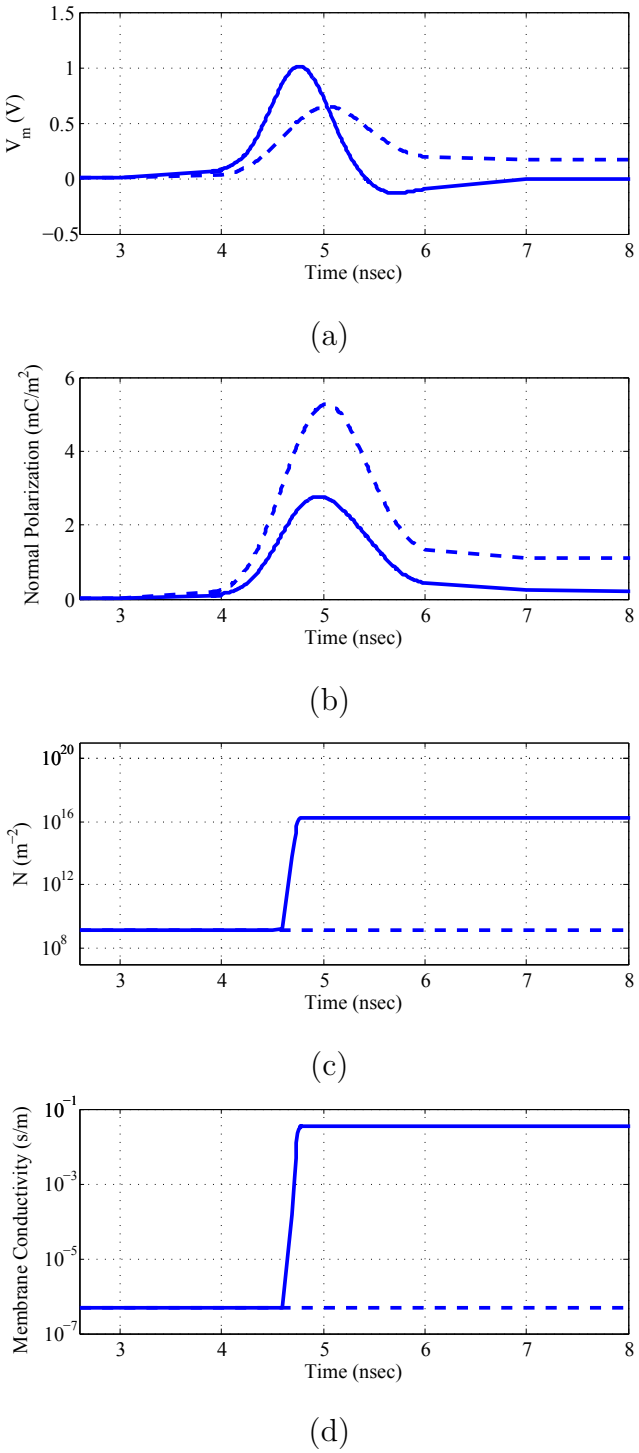

Figure 4.13: *Time response of (a) the transmembrane voltage, (b) the normal polarization, (c) the pore density, and (d) the membrane conductivity at the top of the cell when a nanosecond electric field of* 65 kV/cm *is applied to the nonlinear model of cell.*

Fig. 4.13 the density of the pores and the membrane conductivity increase rapidly after the onset of electroporation for the dispersive membrane whereas for the nondispersive one they stay at the equilibrium level.

With a 0.94 ns duration pulsed electric field the minimum required amplitude to observe electroporation in the nondispersive model is 120 kV/cm. In the dispersive model electroporation occurs with electric field intensity of 65 kV/cm. The conclusion is that ignoring dispersion leads to 85 percent overestimation of the required electroporating pulse intensity.

Fig. 4.14 shows the transmembrane voltage around the cell for the nonlinear dispersive and nondispersive models when an electric field of 130 kV/cm intensity is applied to the cell. In this case both the dispersive and nondispersive membranes experience electroporation. Fig. 4.15 compares the time responses with and without dispersion at the top of the cell. It is obvious that the amplitude of V_m increases faster in the dispersive model resulting in earlier start of electroporation. The transmembrane voltage goes negative for the dispersive and nondispersive models since they both have high membrane conductivity that accompanies electroporation and, therefore, a small time constant. The temporal change of normal polarization density, P shows weaker polarization of the membrane after the onset of the pulse for the dispersive model which explains higher transmembrane voltage and faster start of electroporation. The normal polarization goes negative at the end of the pulse for the dispersive and nondispersive models; however, for the nondispersive

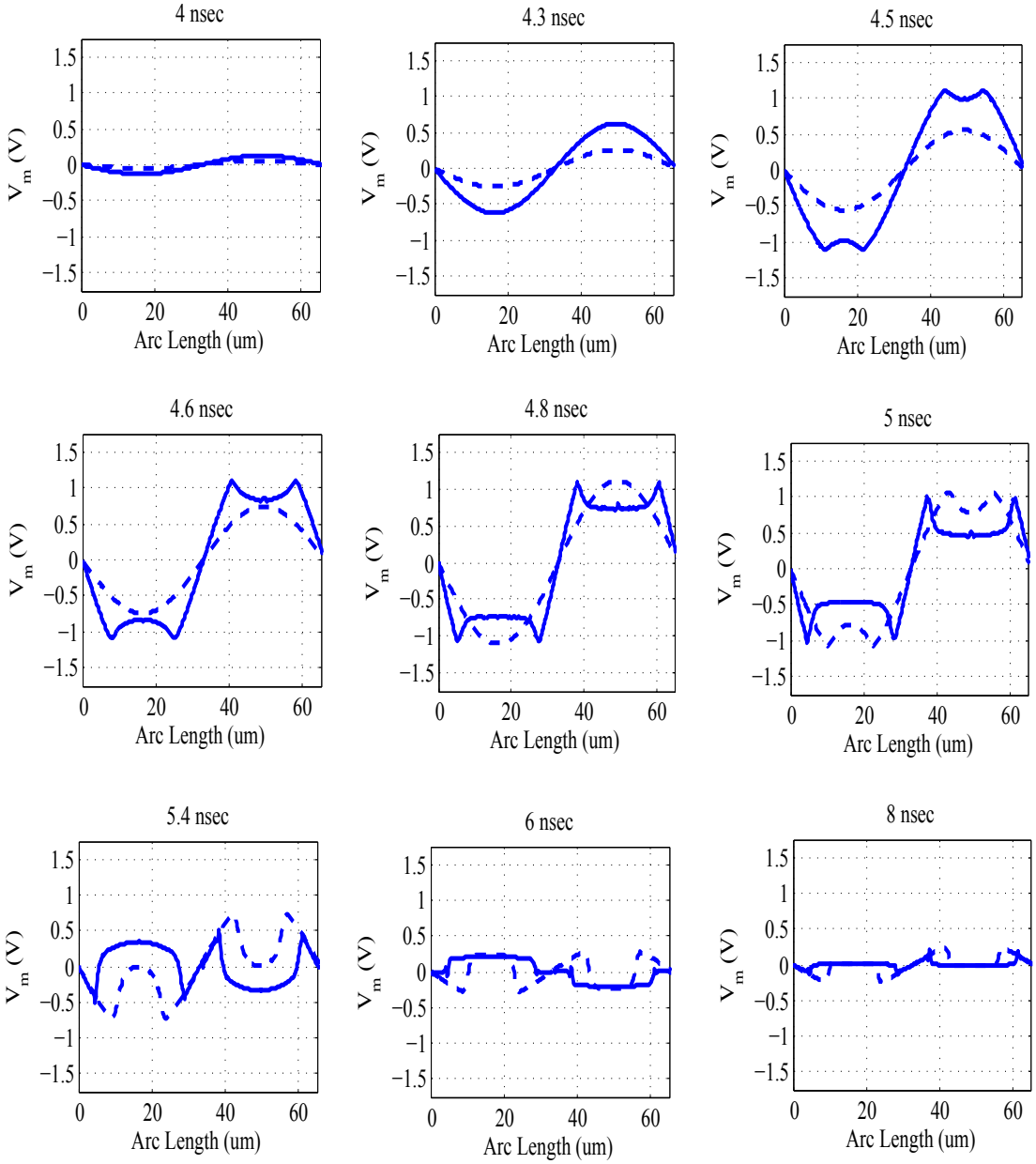

Figure 4.14: *The transmembrane voltage around the cell starting from the right most point on the equator and moving clockwise for the nonlinear dispersive (solid line) and nondispersive (dashed line) models when a* 130 *kV/cm nanosecond electric field is applied to the cell.*

membrane it is in phase with the electric potential across the membrane whereas for the nondispersive membrane it is slightly delayed. The reason is that for a dispersive membrane ϵ in the equation 3.1 is a complex value, incorporating a loss component, number that causes a delay between P and E, while for a nondispersive membrane ϵ is a constant real value. Also, it is noticed that the density of the pores is almost the same for the dispersive and nondispersive models at the areas that poration occurs for both models. Fig. 4.15(c) shows the time course of N with and without dispersion at the top of the cell. In the results reported in [30] the density of the pores in the dispersive model is predicted to exceed that of the nondispersive model. This is different from the result in Fig. 4.15(c). The reason is that in the model of [30] the transmembrane voltage is not controlled by the conduction current of the pores. Therefore, in the dispersive model V_m exceeds the required voltage of electroporation and increases the density of the pores. In our model V_m is limited to approximately 1.1 V by equations (3.11) and (3.10). The density of the pores increases with V_m until the required voltage of electroporation is reached and it stays unchanged afterwards. The ultimate value of N in dispersive and nondispersive models are very close.

Moreover, the dispersive model predicts a wider electroporated area on the membrane surface. As depicted in Fig. 4.16, in the dispersive model the whole surface area of the cell except the equator are experiencing electroporation, while in the nondispersive model only the pole areas are electroporated.

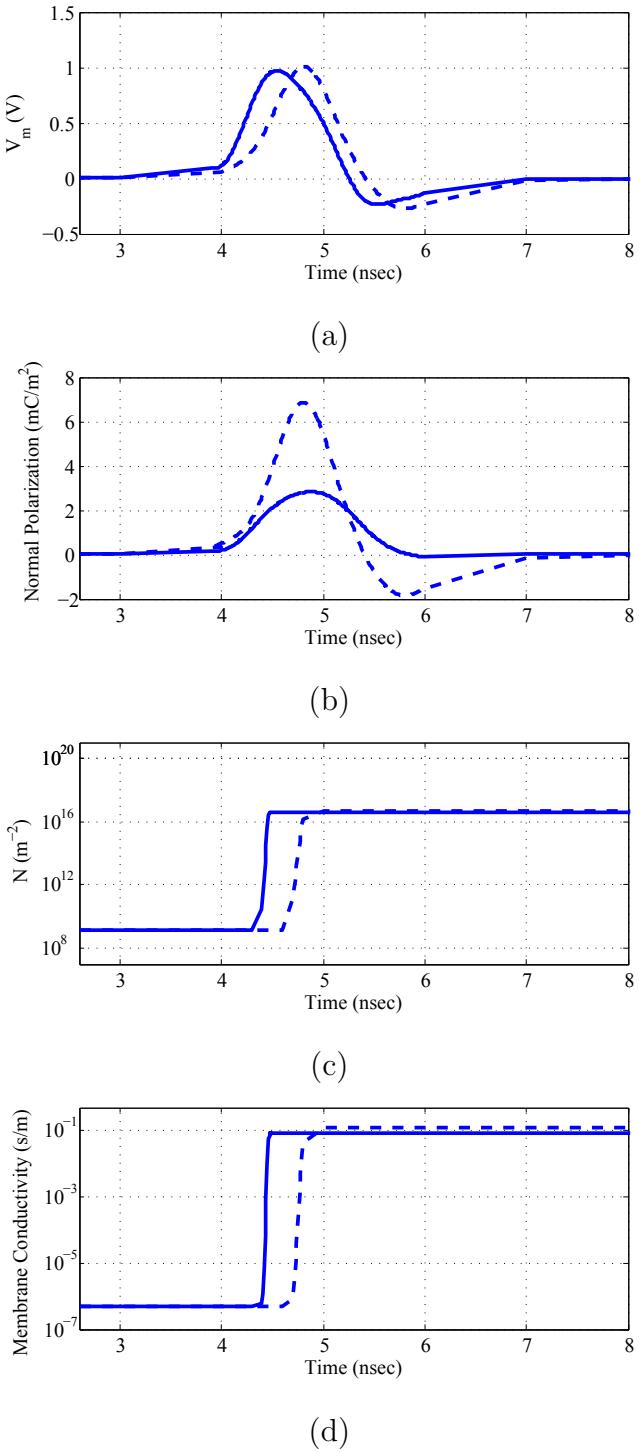

Figure 4.15: *Time course of (a) the transmembrane voltage, (b) the normal polarization, (c) the pore density, and (d) the membrane conductivity at the top of the cell when a nanosecond electric field of* 130 *kV/cm is applied to the nonlinear model of cell.*

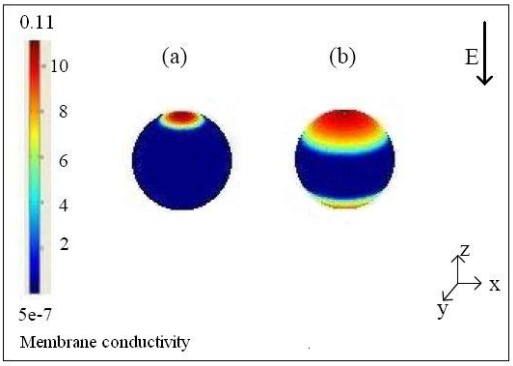

Figure 4.16: *Electroporated area for (a) the dispersive and (b) the nondispersive model at $t = 5$ nsec. The bright color parts are electroporated areas with high conductivity. The color bar shows the conductivity of the membrane.*

In the physical process of electroporation, when the hydrophilic pores are created inside the cell lipid bilayer membrane some polar molecules (e.g. ions and proteins) in the extracellular suspension pass through the membrane and enter the cytoplasm. As a consequence of ion transport across the membrane the cell cytoplasm and membrane conductivity increases. In our model we are accounting only for the increase in the cell membrane conductivity assuming that (i) the pores are created at areas that the transmembrane voltage exceeds the required voltage of electroporation (1.1 V) and (ii) the membrane is very thin such that the diffusion of ions and conductivity increase occur instantaneously. However, the diffusion of ions into the cytoplasm is a more complicated process that needs more insight on the cytoplasm diffusion time constant as well as the volume that is affected inside the cytoplasm.

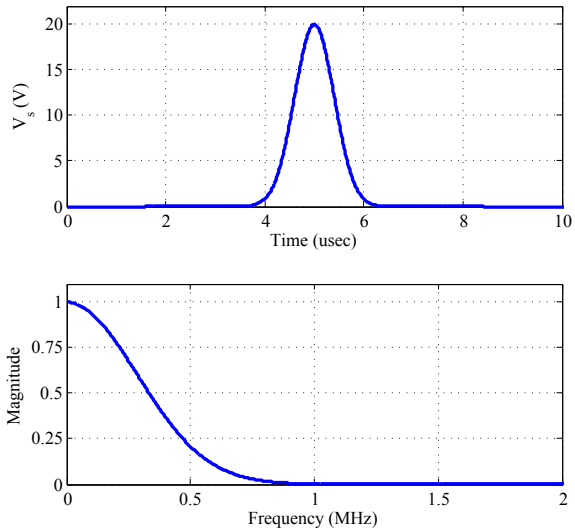

Figure 4.17: *Applied microsecond Gaussian pulsed voltage and its frequency spectral content. The* $10-90\%$ *rise-time of the pulse is* 0.7 μsec *and the peak is at* 5 μsec.

4.4 Cell response to microsecond pulses

We apply a microsecond duration Gaussian pulsed voltage to the top electrode in Fig. 4.1 producing an electric field of 2 kV/cm intensity across the cell at its peak. The geometry and electrical parameters of the cell are the same as previous section. The $10-90\%$ rise-time of the applied pulse is 0.7 μsec and it has a full width at half maximum (FWHM) of 0.94 μsec. The pulse is shown in Fig. 4.17. With microsecond electric pulses the electric response of the cell is effectively determined by the conduction properties of the cytoplasm, membrane, and extracellular medium. Since the frequency spectral content of the applied microsecond pulse is not sufficiently high to cause the dielectric relaxation of the membrane we expect to observe similar behavior for the dispersive and nondispersive models.

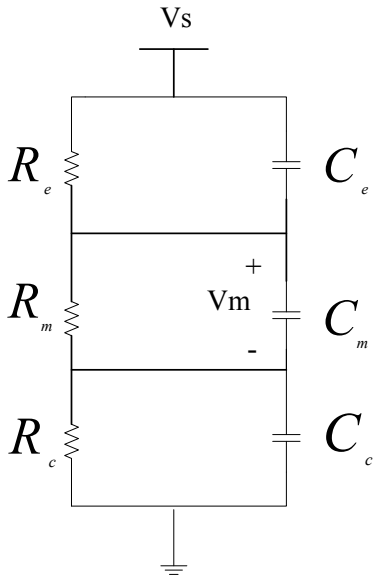

Figure 4.18: *Passive Circuit Model of Cell*

The intensity of the applied microsecond pulse is much lower than the nanosecond pulse used in the previous section. The reason is that with microsecond pulses a greater portion of the total electric potential is across the membrane. Fig. 4.18 shows a passive circuit model of the cell. Assuming one-dimensional resistor and capacitors models, R_j and C_j are defined as

$$R_e = \frac{l_e}{\sigma_e A}, \tag{4.4}$$

$$R_m = \frac{l_m}{\sigma_m A}, \tag{4.5}$$

$$R_c = \frac{l_c}{\sigma_c A}, \tag{4.6}$$

$$C_e = \frac{\epsilon_e A}{d_e}, \tag{4.7}$$

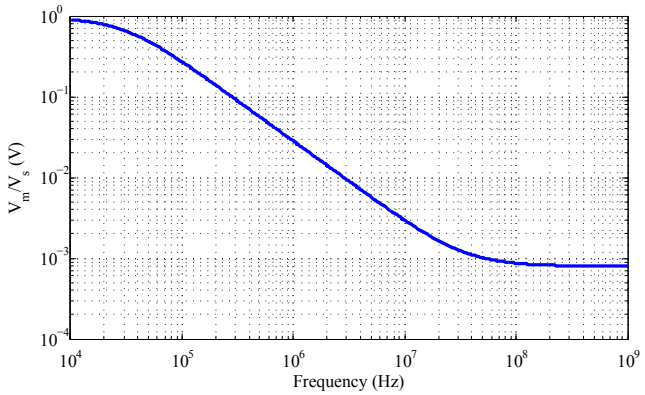

Figure 4.19: $\frac{V_m}{V_s}$ *vs. frequency*

$$C_m = \frac{\epsilon_m A}{d_m}, \tag{4.8}$$

$$C_c = \frac{\epsilon_c A}{d_c} \tag{4.9}$$

where σ_{i0} and ϵ_{i0} are the static conductivity and permittivity of each medium, l is the thickness of each medium and A is the effective cross-sectional area. Fig. 4.19 shows the ratio of V_m/V_s versus frequency. It is obvious that at low frequencies the applied electric potential difference is mostly across the membrane whereas at high frequencies the ratio V_m/V_s is very small. Thus, nanosecond duration pulses require much higher intensity than microsecond duration pulses to cause cell electroporation.

4.4.1 Linear model response

Fig. 4.20 shows the transmembrane voltage for the linear dispersive and nondispersive models along the circumference of the cell. As expected the dispersive and nondispersive membrane models predict the same transmembrane voltage.

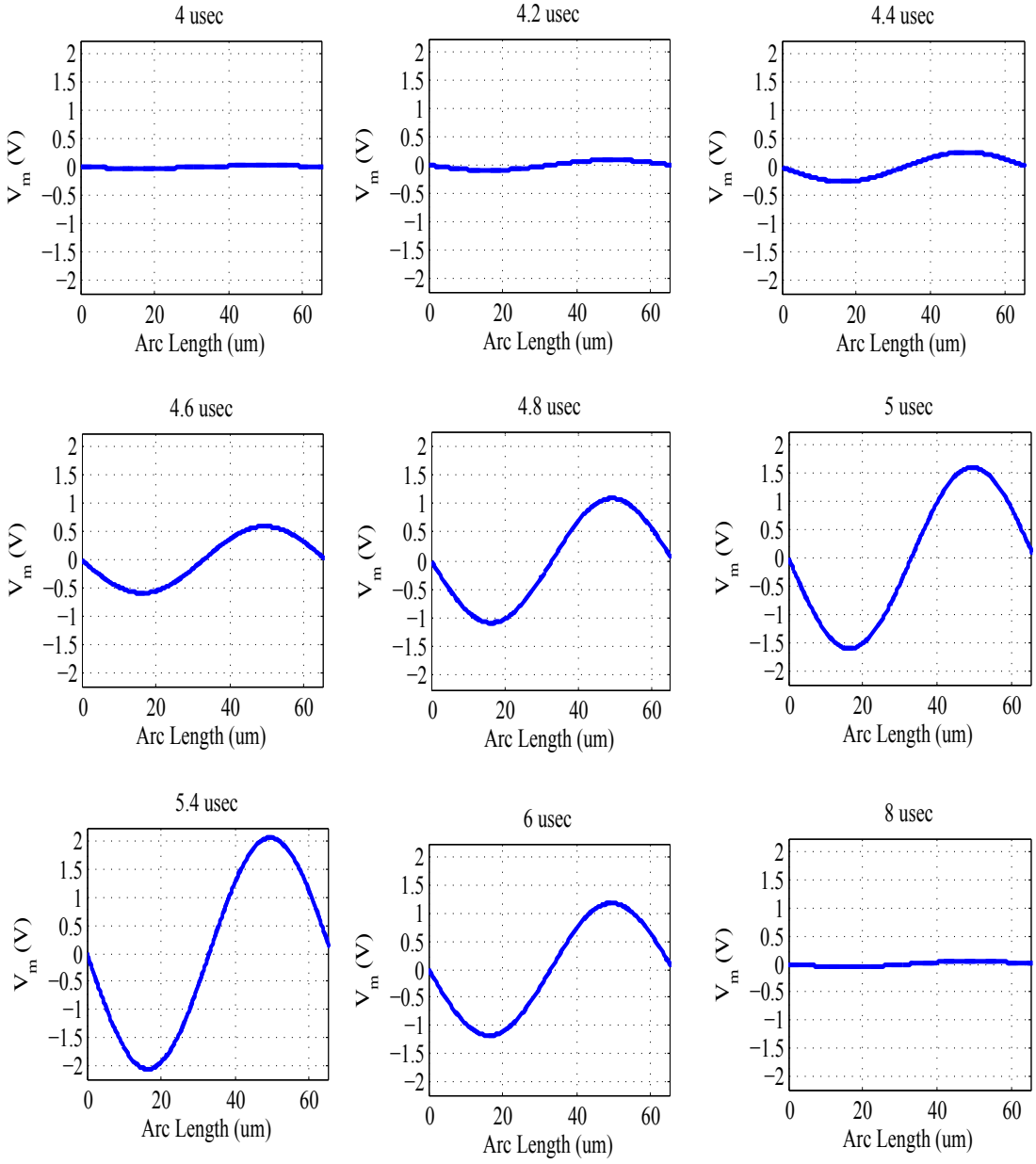

Figure 4.20: *The transmembrane voltage around the cell starting from the right most point on the equator and moving clockwise for the linear dispersive (solid line) and nondispersive (dashed line) models when a 2 kV/cm microsecond electric field is applied to the cell.*

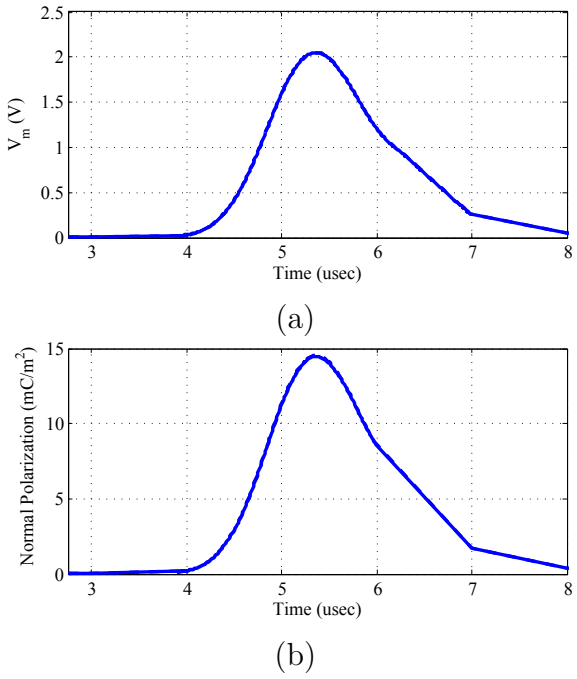

Figure 4.21: *Time course of (a) the transmembrane voltage, (b) the normal polarization, (c) the pore density, and (d) the membrane conductivity at the top of the cell when a microsecond electric field of* 2 *kV/cm is applied to the linear model of cell.*

The time response of the transmembrane voltage and normal polarization at the top point of the cell are shown in Fig. 4.21. It is observed that the peak of the transmembrane voltage is achieved after the peak of the external electric field at 5.4 μsec. The reason for this is that during the applied falling edge of the electric field the cytoplasm and extracellular medium discharge much faster than the membrane (The time constant of a nonporated membrane is in microsecond range while that of the cytoplasm and extracellular medium is in the nanosecond range) and charges the membrane even though the external electric field is decreasing. After 5.4 μsec the membrane starts to discharge decreasing the transmembrane voltage. The time response of the normal polarization, P,

shows that it is completely in phase with the transmembrane voltage, verifying the fact that significant membrane dielectric relaxation does not occur with microsecond duration pulses.

4.4.2 Nonlinear model response

Fig. 4.22 shows the time evolution of the transmembrane voltage along the circumference of the cell. It shows that both the dispersive and nondispersive membranes experience similar electroporation behavior. Electroporation starts at the same time for both models because with the applied microsecond duration pulse significant membrane dielectric relaxation does not occur.

The time response of the transmembrane voltage, normal polarization, pore density, and membrane conductivity at the top point of the cell are shown in Fig. 4.23. Membrane electroporation starts at 4.75 μsec and decreases the transmembrane voltage due to the increase in the membrane conductivity that accompanies electroporation. It is noticed that with microsecond pulses the density of the pores created in the membrane is much smaller than for nanosecond pulses, and is a major difference between conventional electroporation and supra-electroporation. In microsecond electroporation of cells presented in this work we still assumed that pores are created with constant radius of 0.8 nm. More accurate modeling of the phenomenon in the microsecond pulse case requires considering the expansion of the pores.

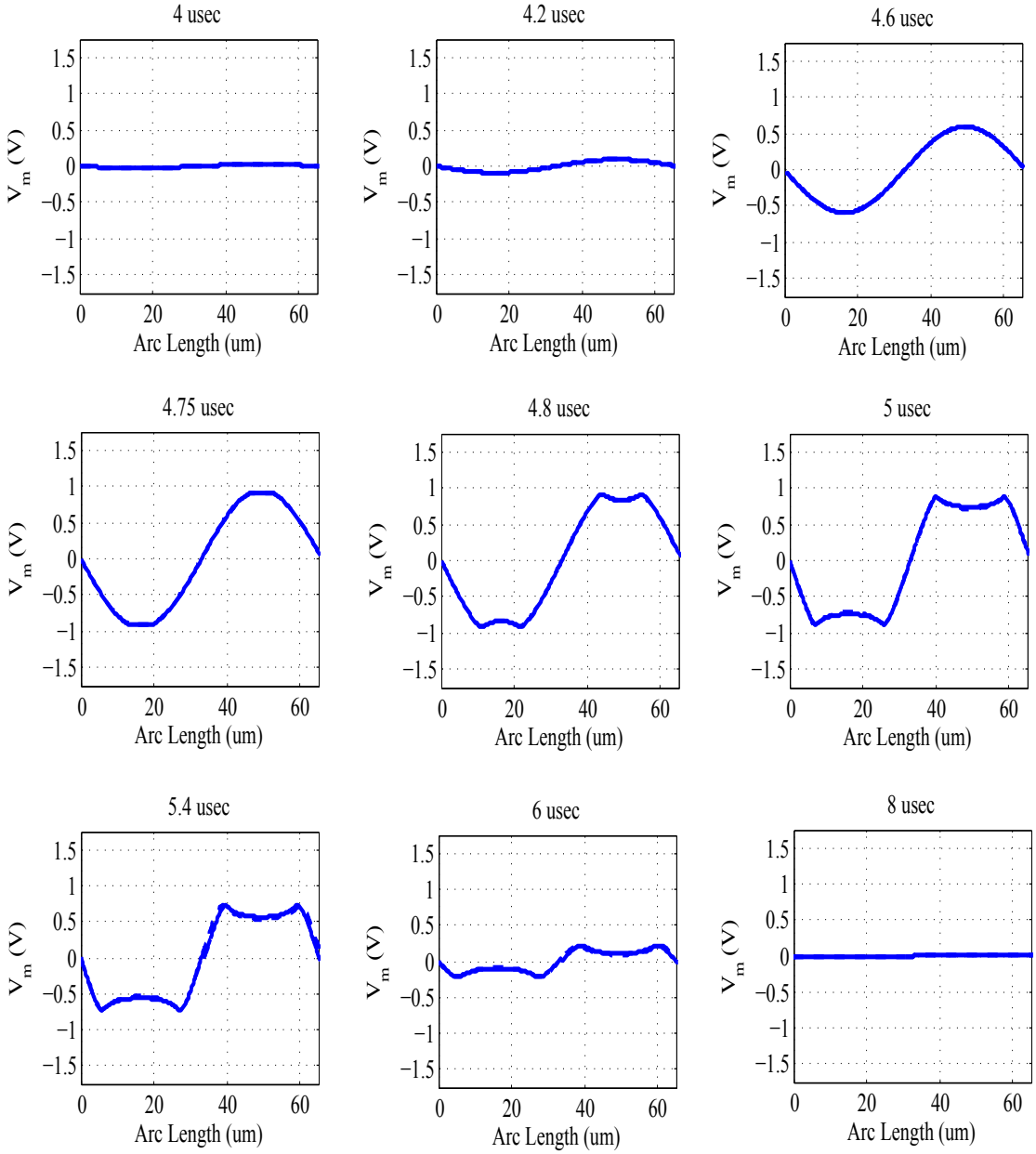

Figure 4.22: *The transmembrane voltage along the circumference of the cell starting from the right most point on the equator and moving clockwise for the nonlinear dispersive (solid line) and nondispersive (dashed line) models when a 2 kV/cm microsecond electric field is applied to the cell.*

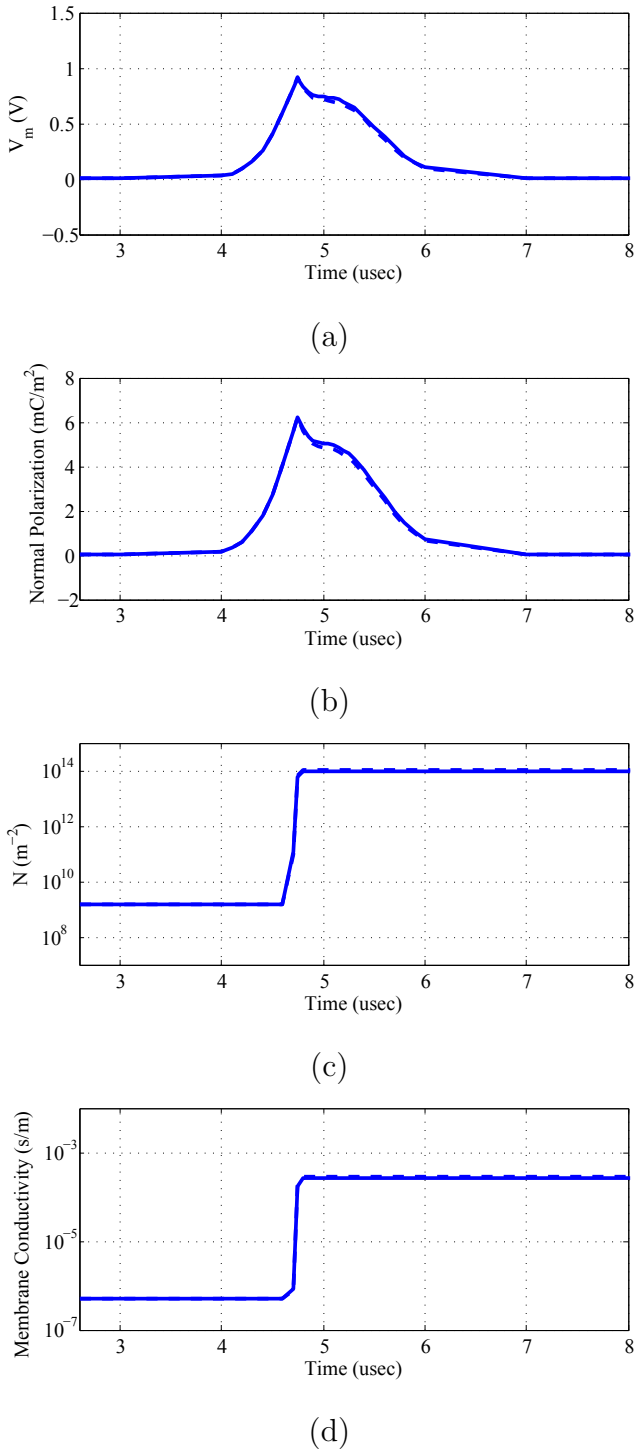

Figure 4.23: *Time course of (a) the transmembrane voltage, (b) the normal polarization, (c) the pore density, and (d) the membrane conductivity at the top of the cell when microsecond electric field of 2 kV/cm is applied to the nonlinear model of the cell.*

4.5 The effect of the pulse fall-time

As mentioned in the previous section, the behavior of the transmembrane voltage at the falling edge of the applied electric pulse is highly dependent on the fall-time of the pulse. For an external electric pulse sufficiently strong to electroporate the cell membrane, the theoretical time constant of the membrane and cytoplasm are

$$\tau_m = \frac{\epsilon_m}{\sigma_m} = \frac{13.9 \times 10^{-12}}{0.04} = 0.35 nsec, \tag{4.10}$$

$$\tau_c = \frac{\epsilon_c}{\sigma_c} = \frac{7.08 \times 10^{-10}}{0.3} = 2.36 nsec. \tag{4.11}$$

where ϵ_m is the high frequency membrane permittivity, σ_m is the conductivity of the membrane after electroporation, ϵ_c is the cytoplasm low frequency permittivity, and σ_c is the static conductivity of the cytoplasm.

In order to investigate the effect of the pulse fall-time on the transmembrane voltage we perform simulations in 2-D space on a simple parallel plate capacitor geometry shown in Fig. 4.24. The top, middle, and bottom layers have the parameters of the extracellular medium, cell membrane, and cytoplasm, respectively. We use the nonlinear dispersive model for the membrane.

Two 100 kV/cm Gaussian rise-time (fall-time) pulses with 1 $nsec$ and 6 $nsec$ fall-time are applied as Vs. Fig. 4.25 shows the applied pulses. The electric potential across the middle layer (membrane) when a 1 $nsec$ rise-time pulse is applied is shown in Fig. 4.25(c).

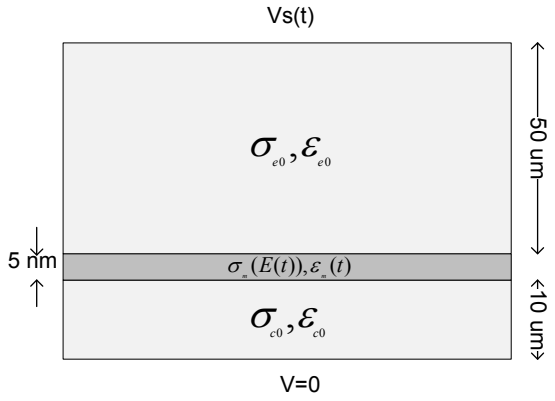

Figure 4.24: *2-D parallel plate capacitor geometry*

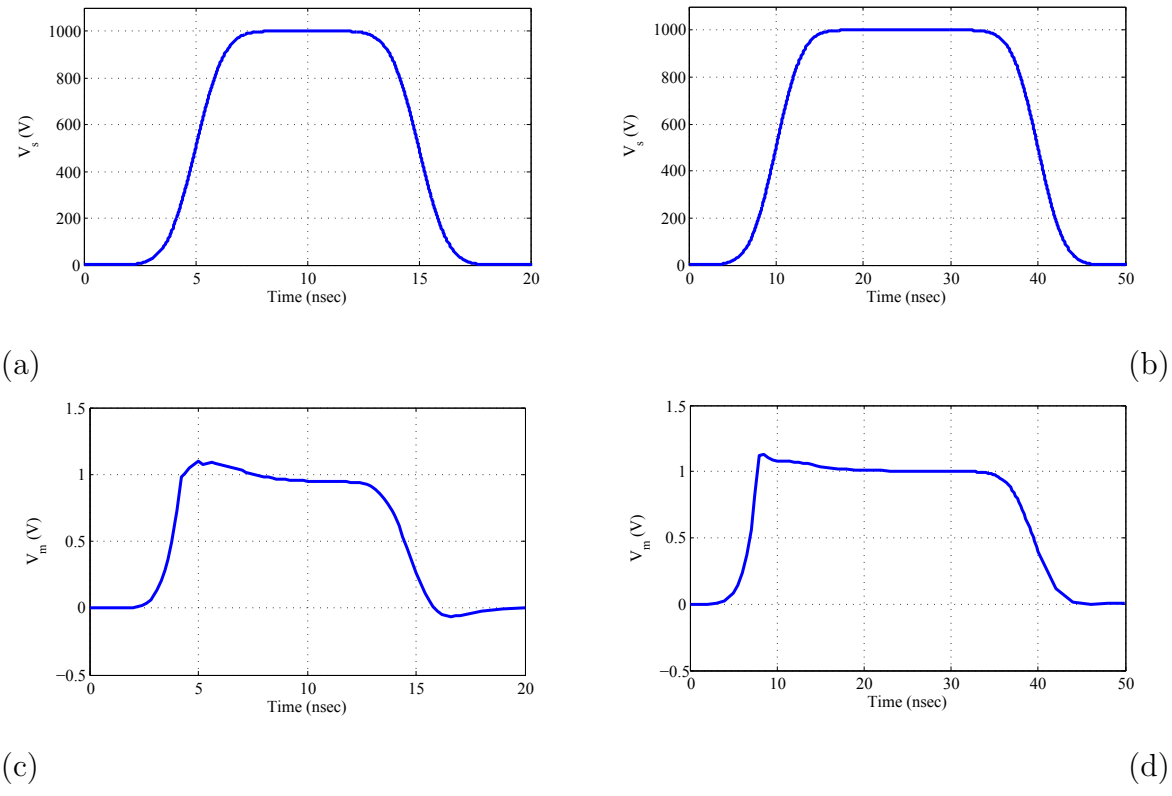

Figure 4.25: *Gaussian (a)* 1 *nsec rise-time,* 10 *nsec duration (b)* 6 *nsec rise-time* 40 *nsec duration pulses applied to the parallel plate structure, and the time response of the electric potential across the middle layer when (c)* 1 *nsec rise-time pulse is applied, and (d)* 6 *nsec rise-time pulse is applied.*

In this case the fall-time of the pulse is shorter than the time constant of cytoplasm and longer than the time constant of membrane. Therefore, the cytoplasm charges the membrane in the opposite direction after the membrane is discharged, causing a negative electric potential across the membrane. Fig. 4.25(d) shows the electric potential across the middle layer (membrane) when a 6 *nsec* rise-time pulse is applied. With a 6 *nsec* rise-time pulse no undershoot is observed in the transmembrane voltage at the falling edge of the electric pulse because both the cytoplasm and membrane have sufficient time to discharge.

Chapter 5

Conclusion and Future Work

5.1 Conclusion

The time course and spatial distribution of the transmembrane voltage is of significant interest in the studies of electroporation of biological cells. The numerical modeling of a cell's response to an external electric field is important since experimental monitoring of the transmembrane voltage is difficult due to the very small time and length scales that the phenomenon occurs. The goal of this research is to improve the electrical model of a cell for applications in nanosecond pulse electroporation. In nanosecond pulse electroporation of cells we need to account for the effect of the dielectric relaxation of the lipid bilayer membrane on the transmembrane voltage. In this project we incorporated the time-domain implementation of the Debye dispersion relation into the nonlinear model of electroporation to predict the transmembrane voltage more accurately. In the presented

model we account for the changes in the membrane conductivity due to the pore conduction as well as changes in the membrane permittivity due to the lipid bilayer membrane dispersion. Comparison of responses of cells to nanosecond pulses determined using the nonlinear dispersive and nondispersive models shows that the increase in the transmembrane voltage and consequently the onset of electroporation occurs faster in the dispersive model when nanosecond pulsed electric field is applied to the cell. Moreover, we noticed that the minimum electric field required to observe electroporation in the cell membrane is significantly reduced when the membrane dispersion is considered.

5.2 Future Work

The nonlinear dispersive model of the cell described in this paper provides more insight on the interaction of high frequency electric pulses with the cell membrane and enables more accurate modeling of nanosecond pulse electroporation of biological cells.

In this research we studied the electrical response of cells to external electric fields assuming a single shell structure for the cells. The study and the proposed nonlinear dispersive model can be extended to multi-shell structures and thus include some of the cell internal organelles. The effect of an external electric field on a cell's internal structures is gaining special interest since it has the potential to open access to the nucleus of the cell. Moreover, in this research we assumed a spherical shape for the cell. Simulations on spherical shape cell provide valuable information on the response of different cell models to

an external electric field. However, it may not provide accurate values for field strengths needed for electroporation. More realistic cell shapes result in more accurate prediction of the cell response. The approach developed here is capable of any arbitrary cell geometry (as long as the radius of membrane curvature is less than its thickness and of the second membrane thickness).

The cell response to an external electric field is highly dependent on the electrical parameters of the cell. In our study we used electrical parameters for CHO cells that have been measured and used in previous studies. Most of the electrical parameters of the cell reported in literatures are based on low frequency measurements. High frequency measurement of the electrical parameters of a cell would lead to more accurate prediction of the cell response to high frequency pulses.

The asymptotic model of electroporation has been developed for conventional electroporation in which the duration of the applied pulse is much longer than the molecular rearrangement time scale and the density of pores formed in the membrane is quiet low. Extending this model for application in nanosecond pulse electroporation would results in more accurate modeling of the phenomenon.

In this research we assumed that pores were created and maintained at the radius of minimum energy. Improving the cell model to incorporate pore expansion will open the door to more advanced modeling of electroporation that could include detailed molecular transport across the membrane.

Bibliography

[1] [Online]. Available: http://www.free-ed.net

[2] [Online]. Available: http://en.wikipedia.org/wiki/File:Phospholipids_aqueous_solution_structures.

[3] [Online]. Available: http://en.wikipedia.org/wiki/File:Pore_schematic.svg

[4] K. C. Smith and J. C. Weaver, "Active mechanisms are needed to describe cell responses to submicrosecond, megavolt-per-meter pulses: Cell models for ultrashort pulses," *Biophysical Journal*, vol. 95, no. 4, pp. 1547 – 1563, 2008.

[5] T. Kotnik and D. Miklavcic, "Theoretical evaluation of voltage inducement on internal membranes of biological cells exposed to electric fields," *Biophysical Journal*, vol. 90, no. 2, pp. 480 – 491, 2006.

[6] D. Miklavcic and T. Kotnik, "Theoretical evaluation of the distributed power dissipation in biological cells exposed to electric fields," *Bioelectromagneticsl*, vol. 21, no. 5, pp. 385 – 394, 2000.

[7] G. Pucihar, D. Miklavcic, and T. Kotnik, "A time-dependent numerical model of transmembrane voltage inducement and electroporation of irregularly shaped cells," *Biomedical Engineering, IEEE Transactions on*, vol. 56, no. 5, pp. 1491 –1501, May 2009.

[8] J. C. Neu and W. Krassowska, "Asymptotic model of electroporation," *Phys. Rev. E*, vol. 59, no. 3, pp. 3471 – 3482, Mar 1999.

[9] D. S. Dimitrov, "Electric field-induced breakdown of lipid bilayers and cell membranes: A thin viscoelastic film mode," *Journal of Membrane Biology*, vol. 78, no. 1, pp. 53–60, 1984.

[10] R. W. Glaser, S. L. Leikin, L. V. Chernomordik, V. F. Pastushenko, and A. I. Sokirko, "Reversible electrical breakdown of lipid bilayers: formation and evolution of pores," *Biochimica et Biophysica Acta (BBA) - Biomembranes*, vol. 940, no. 2, pp. 275 – 287, 1988.

[11] J. C. Weaver and Y. Chizmadzhev, "Theory of electroporation: A review," *Bioelectrochemistry and Bioenergetics*, vol. 41, no. 2, pp. 135 – 160, 1996.

[12] H. Potter, "Electroporation in biology: Methods, applications, and instrumentation," *Analytical Biochemistry*, vol. 144, no. 2, pp. 361–373, 1988.

[13] F. Andr and L. M. Mir, "DNA electrotransfer: its principles and an updated review of its therapeutic applications," *Gene Therapy*, vol. 11, pp. S33–S42, 2004.

[14] J. J. Belehradek, S. Orlowski, L. H. Ramirez, G. Pron, B. Poddevin, and L. M. Mir, "Electropermeabilization of cells in tissues assessed by the qualitative and quantitative electroloading of bleomycin," *Biochimica et Biophysica Acta (BBA) - Biomembranes*, vol. 1190, no. 1, pp. 155 – 163, 1994.

[15] M. Zeira, P. F. Tosi, Y. Mouneimne, J. Lazarte, L. Sneed, D. J. Volsky, and C. Nicolau, "Full-length cd4 electroinserted in the erythrocyte membrane as a long-lived inhibitor of infection by human immunodeficiency virus," *Proceedings of the National Academy of Sciences of the United States of America*, vol. 88, no. 10, pp. 4409–4413, 1991.

[16] B. Gabriel and J. Teissi, "Time courses of mammalian cell electropermeabilization observed by millisecond imaging of membrane property changes during the pulse," *Biophysical Journal*, vol. 76, no. 4, pp. 2158 – 2165, 1999.

[17] "High-throughput and real-time study of single cell electroporation using microfluidics: Effects of medium osmolarity," *Biotechnology and Bioengineering*, vol. 95, no. 6, pp. 1116 – 1125, 2006.

[18] P. T. Vernier, S. Sun, and M. A. Gundersen, "Nanoelectropulse-driven membrane perturbation and small molecule permeabilization," *BMC Cell Biologyy*, vol. 7, p. 37, 2006.

[19] K. Smith, T. Gowrishankar, A. Esser, D. Stewart, and J. Weaver, "The spatially distributed dynamic transmembrane voltage of cells and organelles due to 10 ns pulses: Meshed transport networks," *Plasma Science, IEEE Transactions on*, vol. 34, no. 4, pp. 1394 –1404, 2006.

[20] J. Deng, K. H. Schoenbach, E. S. Buescher, P. S. Hair, P. M. Fox, and S. J. Beebe, "The effects of intense submicrosecond electrical pulses on cells," *Biophysical Journal*, vol. 84, no. 4, pp. 2709 – 2714, 2003.

[21] W. Frey, J. White, R. Price, P. Blackmore, R. Joshi, R. Nuccitelli, S. Beebe, K. Schoenbach, and J. Kolb, "Plasma membrane voltage changes during nanosecond pulsed electric field exposure," *Biophysical Journal*, vol. 90, no. 10, pp. 3608 – 3615, 2006.

[22] K. Schoenbach, S. Xiao, R. Joshi, J. Camp, T. Heeren, J. Kolb, and S. Beebe, "The effect of intense subnanosecond electrical pulses on biological cells," *Plasma Science, IEEE Transactions on*, vol. 36, no. 2, pp. 414 –422, 2008.

[23] Q. Hu and R. P. Joshi, "Transmembrane voltage analyses in spheroidal cells in response to an intense ultrashort electrical pulse," *Phys. Rev. E*, vol. 79, no. 1, p. 11901, Jan 2009.

[24] K. Schoenbach, B. Hargrave, R. Joshi, J. Kolb, R. Nuccitelli, C. Osgood, A. Pakhomov, M. Stacey, R. Swanson, J. White, S. Xiao, J. Zhang, S. Beebe, P. Blackmore, and E. Buescher, "Bioelectric effects of intense nanosecond pulses," *Dielectrics and Electrical Insulation, IEEE Transactions on*, vol. 14, no. 5, pp. 1088 –1109, 2007.

[25] H. Xu, P. D. Nallathamby, and X.-H. N. Xu, "Real-time imaging and tuning subcellular structures and membrane transport kinetics of single live cells at nanosecond regime," *The Journal of Physical Chemistry B*, vol. 113, no. 43, pp. 14 393–14 404, 2009.

[26] T. Kotnik, D. Miklavcic, and T. Slivnik, "Time course of transmembrane voltage induced by time-varying electric fields–a method for theoretical analysis and its application," *Bioelectrochemistry and Bioenergetics*, vol. 45, no. 1, pp. 3 – 16, 1998.

[27] C. Yao, D. Mo, C. Li, C. Sun, and Y. Mi, "Study of transmembrane potentials of inner and outer membranes induced by pulsed-electric-field model and simulation," *Plasma Science, IEEE Transactions on*, vol. 35, no. 5, pp. 1541 –1549, oct. 2007.

[28] V. Vajrala, J. R. Claycomb, H. Sanabria, and J. H. M. Jr., "Effects of oscillatory electric fields on internal membranes: An analytical model," *Biophysical Journal*, vol. 94, no. 6, pp. 2043 – 2052, 2008.

[29] K. A. DeBruin and W. Krassowska, "Modeling electroporation in a single cell. i. effects of field strength and rest potential," *Biophysical Journal*, vol. 77, no. 3, pp. 1213 – 1224, 1999.

[30] C. Merla, A. Paffi, M. Liberti, F. Apollonio, F. Danei, P. Leveque, and G. d'Inzeo, "Nanosecond pulsed electric field (nspef): A microdosimetry study at single cell level," in *Electromagnetics in Advanced Applications, 2009. ICEAA '09. International Conference on*, 2009, pp. 909 –912.

[31] J. E. Hall and A. C. Guyton, *Textbook of Medical Physiology*. Philadelphia: Elsevier Saunders, 2006.

[32] K. C. Melikov, V. A. Frolov, A. Shcherbakov, A. V. Samsonov, Y. A. Chizmadzhev, and L. V. Chernomordik, "Voltage-induced nonconductive pre-pores and metastable single pores in unmodified planar lipid bilayer," *Biophysical Journal*, vol. 80, no. 4, pp. 1829 – 1836, 2001.

[33] P. Vernier, Y. Sun, L. Marcu, C. M. Craft, and M. A. Gundersen, "Nanosecond pulsed electric fields perturb membrane phospholipids in t lymphoblasts," *FEBS*

Letters, vol. 572, no. 1-3, pp. 103 – 108, 2004.

[34] K. T. Powell and J. C. Weaver, "Transient aqueous pores in bilayer membranes: A statistical theory," *Bioelectrochemistry and Bioenergetics*, vol. 15, no. 2, pp. 211 – 227, 1986.

[35] B. Klosgen, C. Reichle, S. Kohlsmann, and K. Kramer, "Dielectric spectroscopy as a sensor of membrane headgroup mobility and hydration," *Biophysical Journal*, vol. 71, no. 6, pp. 3251 – 3260, 1996.

[36] S. Garcia, R. Rubio, A. Bretones, and R. Martin, "Extension of the adi-fdtd method to debye media," *Antennas and Propagation, IEEE Transactions on*, vol. 51, no. 11, pp. 3183 – 3185, 2003.

[37] A. Grunbaum, S. Petersen, H. W. Pau, and U. Riene, "Thin membrane modelling for the electrical stimulation of auditory nerve," in *Proceedings of the COMSOL Conference 2009 Milan*, 2009.

[38] E. Salimi, G. Bridges, and D. Thomson, "The effect of dielectric relaxation in nanosecond pulse electroporation of biological cells," in *Antenna Technology and Applied Electromagnetics the American Electromagnetics Conference (ANTEM-AMEREM), 2010 14th International Symposium on*, 2010, pp. 1 –4.

Appendix

Appendix A

Hydrophobic and Hydrophilic Pore Energy

The energy of a hydrophobic pore is defined as the change in the membrane energy that results from the formation of a hydrophobic pore of radius r in the membrane. The energy of a hydrophobic pore at the transmembrane voltage $V_m = 0$ is calculated from [10]

$$E_o(r) = 2\pi h \sigma_0 r \frac{I_1(r/\rho)}{I_0(r/\rho)}, \tag{A.1}$$

where $I_n(x)$ are $n-th$ order Bessel functions, h is the thickness of the membrane, σ_0 is the interface tension between hydrophobic lipid tails and water, ρ is a constant, and r is the radius of the hydrophobic pore.

The energy of a hydrophilic pore is defined as the change in the membrane energy that results from the formation of a hydrophilic pore of radius r in the membrane. The

Table A.1: *The hydrophobic and hydrophilic energy parameters [8].*

Parameter	Symbol	Value
Thickness of the membrane	h	$5\ nm$
Interface tension between hydrophobic tails and water	σ_0	$0.05\ N/m$
Constant in Eq. A.1	ρ	$1\ nm$
Energy per unit length of the pore perimeter	γ	$1.8 \times 10^{-11}\ J/m$
Energy per unit area of an intact membrane	σ	$10^{-3}\ J/m^2$
Constant in Eq. A.2	C	$9.67 \times 10^{-15}\ J^{\frac{1}{4}m}$

energy of a hydrophilic pore at the transmembrane voltage $V_m = 0$ is calculated from [8]

$$E_i(r) = 2\pi\gamma r - \pi\sigma r^2 + \left(\frac{C}{r}\right)^4, \tag{A.2}$$

where γ is the energy per unit length of the pore perimeter, σ is the energy per unit area of an intact membrane, C is a constant, and r is the radius of the hydrophilic pore. The value of the hydrophobic and hydrophilic energy parameters are given in Table A.1 [8].

When the transmembrane voltage is elevated, the energy of hydrophobic and hydrophilic pores are calculated from [10]

$$E(r, V_m) = E_0(r) - \frac{\pi}{2h}(\epsilon_{rw} - \epsilon_{rm})\epsilon_0 V_m^2 r^2, \tag{A.3}$$

where $E_0(r)$ is the pore energy at $V_m = 0$, ϵ_{rw} is the dielectric constant of water, ϵ_{rm} is the dielectric constant of the membrane and V_m is the transmembrane voltage. It is assumed that the energy of both hydrophilic and hydrophobic pores change the same with the transmembrane voltage. Therefore, r_*, the pore radius at which hydrophobic and

hydrophilic pores have the same energy, does not depend on the transmembrane voltage.